

A General View on Double Limits in Differential Equations

Christian Kuehn,^{1,2} Nils Berglund,³ Christian Bick,^{4,5,6} Maximilian Engel,⁷ Tobias Hurth,⁸ Annalisa Iuorio,⁹ and Cinzia Soresina¹⁰

¹*Department of Mathematics, Technical University of Munich, Boltzmannstr. 3, 85748 Garching b. München, Germany*

²*Complexity Science Hub Vienna, Josefstädter Str. 39, 1080 Vienna, Austria*

³*Institut Denis Poisson (IDP), Université d'Orléans, Université de Tours, CNRS – UMR 7013, Bâtiment de Mathématiques, B.P. 6759, 45067 Orléans Cedex 2, France*

⁴*Department of Mathematics, Vrije Universiteit Amsterdam, De Boelelaan 1111, Amsterdam, the Netherlands*

⁵*Department of Mathematics, University of Exeter, Exeter EX4 4QF, UK*

⁶*Institute for Advanced Study, Technical University of Munich, Lichtenbergstr. 2, 85748 Garching, Germany*

⁷*Department of Mathematics, Freie Universität Berlin, Arnimallee 6, 14195 Berlin, Germany*

⁸*Institut de mathématiques, Université de Neuchâtel, Rue Emile-Argand 11, CH-2000 Neuchâtel*

⁹*Faculty of Mathematics, University of Vienna, Oskar-Morgenstern-Platz 1, 1090, Vienna, Austria*

¹⁰*Institute for Mathematics and Scientific Computing, University of Graz, Heinrichstr. 36, 8010 Graz, Austria*

(Dated: March 17, 2022)

In this paper, we review several results from singularly perturbed differential equations with multiple small parameters. In addition, we develop a general conceptual framework to compare and contrast the different results by proposing a three-step process. First, one specifies the setting and restrictions of the differential equation problem to be studied and identifies the relevant small parameters. Second, one defines a notion of equivalence via a property/observable for partitioning the parameter space into suitable regions near the singular limit. Third, one studies the possible asymptotic singular limit problems as well as perturbation results to complete the diagrammatic subdivision process. We illustrate this approach for two simple problems from algebra and analysis. Then we proceed to the review of several modern double-limit problems including multiple time scales, stochastic dynamics, spatial patterns, and network coupling. For each example, we illustrate the previously mentioned three-step process and show that already double-limit parametric diagrams provide an excellent unifying theme. After this review, we compare and contrast the common features among the different examples. We conclude with a brief outlook, how our methodology can help to systematize the field better, and how it can be transferred to a wide variety of other classes of differential equations.

1. INTRODUCTION

Effectively all problems arising from science and engineering are studied by only considering a suitably reduced model of reality. In particular, we would often like to reduce differential equations by assuming that certain physical effects or external influences do not play a major role for the scientific question of interest. Yet, this implicitly supposes we can also show that the terms we do neglect are in some sense “small” so that they do not change the answers to the relevant scientific questions. There is a vast number of differential equations, where we are faced with trying to prove that certain terms do not influence our results. In each problem, we usually have small parameters, which control the strength of the terms we want to neglect. Some typical examples appearing in the context of differential equations are:

- *Time Scale Separation:* Two, or more, sets of variables evolve at different rates.
- *Noise Level:* Finite-size effects or external forces are modeled via noise.
- *Spatial Scale Separation:* Two, or more, sets of vari-

ables have differing spatial scales.

- *Network Coupling:* Operating a system within a network leads to new coupling dependencies.

In this paper, we are going to focus on these areas to illustrate the types of results one can obtain for (multiple) small parameters. Of course, there are many other areas in differential equations, where small parameters appear, for example:

- *Discretization Size:* Temporal and/or spatial discretization leads to small parameters.
- *Inverse Particle Number:* One wants to convert finite systems to a continuum model.
- *Interfaces:* Interfaces or boundary layers are often small.
- *Nonlocal Coupling:* Local derivatives are augmented by global integral terms.
- *Nonsmoothness:* Functions are taken smooth outside of small subsets of space.

- *Time Delay*: (Small) communication delay induces a time history dependence.
- *Near-Symmetry*: A system might be very close to a symmetric one.
- *Near-Integrability*: Perturbations of integrable and/or Hamiltonian systems are well-studied.

Even the combination of the two previous lists is just a restricted snapshot of all potential cases where small parameters may appear. From a historical perspective, small parameters in differential equations are a quite classical topic that can be traced back at least to the end of the 19th century. Among the first applications were celestial mechanics [189] and fluid dynamics [191]. In celestial mechanics, since the two-body problem is often easily solvable, the three-body problem naturally lends itself to consider singular perturbations by assuming two large mass bodies and one very small mass. In fluid mechanics, assuming very large viscosity is helpful as this assumption usually precludes the existence of turbulent flow. In the limited space of this work, it is impossible to give proper credit to the very successful, long, and sometimes winding, history of singular perturbations in celestial mechanics and fluid dynamics, so we refer to [37, 108, 182, 208] containing excellent historical accounts and references regarding the development of these areas.

Within the 20th century, the use of small parameters and perturbation techniques for differential equations have permeated effectively all areas of science and engineering, while more recently also quantitative modelling in the social sciences tends to rely on differential equation modelling. For some pointers to the vast literature, we refer to the books [25, 27, 107, 122, 128, 133, 145, 177, 181, 186, 193, 209, 213, 214], where classical cases of ordinary and partial differential equations (ODEs and PDEs) with one small parameter are considered from a number of different viewpoints.

Although the literature is quite detailed, it has become apparent in recent years that several techniques have to be extended to deal with more complex 21st century challenges, where differential equations and small parameters still take center stage. First, one might wonder, why existing methods have to be developed further? The first key reason is that mathematical modeling of complex systems almost immediately dictates that the case of just one small parameter is very rare. For example, it would be very difficult to argue that global climate dynamics, socio-economic networked systems, or neuro-mechanical as well as systems biology problems, frequently contain just *one* small parameter. Second, in complex systems we often deal with many instabilities. Each instability, even if it is localized in parameter and phase space, leads to a delicate balance between nonlinear terms. Hence, we cannot invoke simple principles that very stable leading-order linear terms dominate so that small contributions from external/internal model perturbations are irrelevant. This entails the need for

larger phase and parameter spaces [144]. In summary, there is an imminent need to study the case of two or more small parameters carefully to obtain a good practical understanding of current important topics differential equations.

As one might expect, this field also has some history within several sub-disciplines of differential equations. Among the most classical cases, where two small parameters have been analyzed first, were ODEs with a focus on direct asymptotic methods such as matching [92, 169, 179, 180], although more recently also more geometric ODE approaches have gained popularity, see e.g. [56, 139, 140, 147]. Although extensions of existing approaches are often key components for our understanding of multiple small parameters, the development is not nearly as systematic and detailed as for just one distinguished small parameter. One can view the situation in analogy with several other areas of differential equations, e.g., second-order scalar oscillators already show a lot of interesting behaviour but eventually one has to go beyond a widely accepted standard class. Therefore, we believe it is now time to re-think and systematize double limits in differential equations. In fact, virtually within all areas of differential equations, multiple small parameters do appear. In this review, we try to reflect this broader perspective via several illustrating examples motivated by very different applications. We are going to describe many key challenges, where a naive direct approach of taking double limits fails.

More precisely, a common, yet highly non-trivial, situation we want to understand are doubly-singularly perturbed differential equations, or more generally multi-scale dynamics with multiple small parameters. As argued above, already a unified framework to understand doubly-singular perturbations is still lacking so this will be our starting point. Here we make a conceptual step towards improving this situation.

Consider a doubly-singularly perturbed differential equation with two small non-negative parameters ε and δ . Often we are interested in the local behavior of the differential equation in the cone

$$\mathcal{K} := \{(\varepsilon, \delta) \in \mathbb{R}^2 : \varepsilon \geq 0, \delta \geq 0\}$$

intersected with a sufficiently small ball around the origin. The natural step is to try to partition \mathcal{K} into different regions as shown in Figure 1. To make such a partitioning precise, we propose several steps:

- (S1) Specify the setting and restrictions of the problem \mathcal{X} to be studied.
- (S2) Define a notion of equivalence via a property/observable \mathcal{P} for the partitioning.
- (S3) Study the possible asymptotic limit problems \mathcal{A} to complete the diagram.

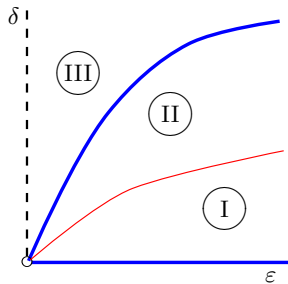


FIG. 1: Sketch of a partitioning of the positive quadrant \mathcal{K} near the doubly-singular limit $\varepsilon \rightarrow 0$ and $\delta \rightarrow 0$ into three different regions (I)–(III), which are non-equivalent under a property \mathcal{P} . The thick lines (in blue) indicate hard boundaries between the different regions, e.g. between (II) and (III) there is a precise curve separating these regions. The thin line (in red) indicates that the boundary is only asymptotic up to a constant between two regions. Dashed lines (in black) indicate an unclassified axis (such as the vertical axis in this figure). The circle at the origin also means that at this point a classification with respect to \mathcal{P} is not known and/or may not even be possible.

In the available literature, these steps can be found in various incarnations and various levels of mathematical rigor. What tends to be missing in many problems is to *recognize* (S1)–(S3) in a clear way to allow for a more *comparative* and *systematic* classification of possible behaviors. Already very simple classical examples, as discussed in Section 2, show that missing small details or slight changes in the setting \mathcal{X} or definition \mathcal{P} in the steps (S1)–(S2) can lead to completely different answers. We are going to show in this work that if the steps (S1)–(S3) are carried out carefully and within a uniform framework, a surprisingly coherent picture emerges, how doubly-singularly perturbed differential equations can be studied. The cross-connections between different classes of effects and methods become more visible. Universal classification diagrams emerge that concisely make the differences and similarities between different sub-fields of differential equations visible. Hence, a systematic study of doubly-singular limits can be viewed as another unifying scientific principle in the analysis of differential equations.

The remaining part of this paper is structured as follows: In Section 2, we explain our approach via simple examples from analysis and algebra without a direct reference to differential equations. The core part of this work is contained in Section 3, where numerous classes of known results for differential equation problems are re-cast precisely in the three steps (S1)–(S3) to provide a general framework, which highlights the unity of area. This includes problems from fast-slow ODE dynamics, small noise stochastic differential equations (SDEs) and piecewise deterministic Markov processes (PDMPs), spatial problems arising from the bifurcation analysis of partial differential equations (PDEs), and a problem in large-scale network dynamics. In Section 4, we then contrast

and compare the results. Section 5 provides an outlook towards a more systematic study of multi-parameter singular limits for differential equations.

2. CLASSICAL EXAMPLES

Before starting with the development of a singular limit analysis of various classes of differential equations, we illustrate some basic principles that occur in the steps (S1)–(S3) in simpler settings.

2.1. Elementary Algebra

Consider the root-finding problem of a very simple quadratic polynomial

$$f(x; \varepsilon, \delta) := \varepsilon x^2 - \delta \stackrel{!}{=} 0. \quad (\mathcal{X}_{\text{rts}})$$

For the problem $(\mathcal{X}_{\text{rts}})$, we assume that we do not allow any coordinate changes and/or preliminary algebraic scaling operations for the problem, i.e., we want to find the roots as is. For any $\varepsilon, \delta > 0$, we have the roots $x_{\pm} = \pm\sqrt{\delta/\varepsilon}$. Now it crucially depends on the choice of the property \mathcal{P} what a classification diagram in a form similar to Figure 1 would look like. Suppose we take as a definition that two problems of the form $(\mathcal{X}_{\text{rts}})$ are equivalent if they have the same property

$$\mathcal{P}_{[-1,1]} := \text{cardinality}\{x \in [-1, 1] : f(x; \varepsilon, \delta) = 0\},$$

where we count roots according to multiplicity. Then one just calculates $|x_{\pm}|^2 = \delta/\varepsilon \leq 1$ which yields $\delta \leq \varepsilon$. Hence, there are just two regions in the (ε, δ) -diagram separated by the diagonal $\{\delta = \varepsilon\} \cap \mathcal{K}$. Above the diagonal, we have $\delta > \varepsilon$ so $\mathcal{P}_{[-1,1]}|_{\delta > \varepsilon} = 0$, while on or below the diagonal we have $\mathcal{P}_{[-1,1]}|_{\delta \leq \varepsilon} = 2$. Of course, the point at the origin is special leading to a solution set which is uncountable so we decide to leave it out in our classification; see Figure 2.

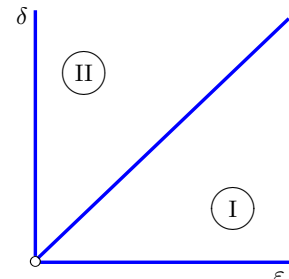


FIG. 2: Classification diagram with respect to the property $\mathcal{P}_{[-1,1]}$. In region II we have no zeros while in region I we have two zeros (counting multiplicity).

The splitting into two main regions is also visible via considering the two singular limit problems of $(\mathcal{X}_{\text{rts}})$,

namely

$$\lim_{\varepsilon \rightarrow 0} f(x; \varepsilon, \delta) = -\delta \stackrel{!}{=} 0, \quad (\mathcal{A}_{\text{rts}}^{\varepsilon=0})$$

and

$$\lim_{\delta \rightarrow 0} f(x; \varepsilon, \delta) = \varepsilon x^2 \stackrel{!}{=} 0, \quad (\mathcal{A}_{\text{rts}}^{\delta=0})$$

where we get no roots and a double-root respectively. In summary, there is also an inherent non-commutativity in the limits. Yet, the precise setting of $(\mathcal{X}_{\text{rts}})$ and the specification $\mathcal{P}_{[-1,1]}$ are crucial. For example, if we use $\mathcal{P}_{\mathbb{R}}$ instead, looking for all the real roots, then there is only one naturally singular line remaining in parameter space given by $\{\varepsilon = 0, \delta > 0\}$ with no roots and the usual singular situation at the point $(\varepsilon, \delta) = (0, 0)$. Also, given the function

$$f(x; \varepsilon, \delta) := \varepsilon x^2 - \delta \quad (1)$$

we could have used a completely different property \mathcal{P} to check for equivalence. For example, we could ask for a binary classification and set

$$\mathcal{P}_{\text{cvx}} = \begin{cases} 1 & \text{if } f \text{ is convex in } x, \\ 0 & \text{if } f \text{ is not convex in } x. \end{cases} \quad (2)$$

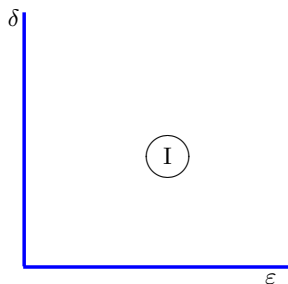


FIG. 3: Classification diagram with respect to the property \mathcal{P}_{cvx} . We just have a single region as $f(x; \varepsilon, \delta) = \varepsilon x^2 - \delta$ is always convex on \mathcal{K} .

Then we always have $\mathcal{P}_{\text{cvx}}|_{(\varepsilon, \delta) \in \mathcal{K}} = 1$ so the singular limit classification is somewhat trivial as shown in Figure 3. This demonstrates that, although many a-priori natural looking mathematical properties could be used for double limits, it is vital to have a good motivation from applications and modeling to select the most important ones.

2.2. Elementary Analysis

The issues illustrated in the last section are evidently not limited to just purely algebraic problems. For example, let us consider the classical function

$$\tilde{f}(x, y) := \begin{cases} \frac{xy(x^2 - y^2)}{x^2 + y^2} & \text{if } (x, y) \neq (0, 0), \\ 0 & \text{if } (x, y) = (0, 0), \end{cases} \quad (\mathcal{X}_{\text{partials}})$$

which is known to be a simple counter-example in the context of Schwarz's Theorem since the partial derivatives do not commute at zero

$$-1 = \partial_{xy} \tilde{f}(0, 0) \neq \partial_{yx} \tilde{f}(0, 0) = 1. \quad (3)$$

Evidently, we can also just understand this via double limits in defining

$$f(x, y; \varepsilon, \delta) := \frac{\tilde{f}(x+\varepsilon, y+\delta) - \tilde{f}(x, y+\delta)}{\varepsilon \delta} + \frac{\tilde{f}(x, y) - \tilde{f}(x+\varepsilon, y)}{\varepsilon \delta},$$

and then (3) just means that

$$\lim_{\delta \rightarrow 0} \lim_{\varepsilon \rightarrow 0} f(x, y; \varepsilon, \delta) \neq \lim_{\varepsilon \rightarrow 0} \lim_{\delta \rightarrow 0} f(x, y; \varepsilon, \delta)$$

if we evaluate the two limits at $(x, y) = (0, 0)$. Evidently the subdivision of the cone \mathcal{K} again depends crucially on the choice of the property \mathcal{P} . However, here we shall fix the relevant property via second partial derivatives below.

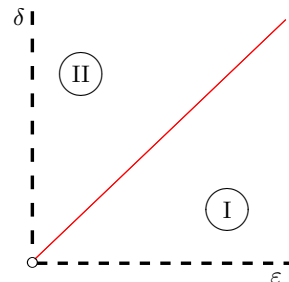


FIG. 4: Classification diagram with respect to the property $\mathcal{P}_{\partial\partial}$. The two regions correspond to the two possible partial derivative values at the origin of the function $(\mathcal{X}_{\text{partials}})$ given for our elementary analysis problem. The thin line (red) could have been chosen at any fixed slope as it is an asymptotic subdividing line of the form $\{\delta = \kappa\varepsilon, \varepsilon > 0\}$ for some fixed constant $\kappa > 0$.

Since we are in an analytic setting, and not in an algebraic one, it often makes sense not to aim for a point-wise subdivision of the cone \mathcal{K} . Instead, we are going to use an asymptotic subdivision by assuming that $\delta = \delta(\varepsilon)$ with $\delta \in \mathbb{C}^0(\mathbb{R}_0^+, \mathbb{R}_0^+)$ and $\delta(0) = 0$, which just means that δ is a continuous function of ε vanishing simultaneously. If we define

$$\mathcal{P}_{\partial\partial} := \lim_{\varepsilon \rightarrow 0} f(x, y; \varepsilon, \delta(\varepsilon))|_{(x, y) = (0, 0)}$$

then there are two main regions in \mathcal{K} . Either we have $\delta(\varepsilon) = o(\varepsilon)$ as $\varepsilon \rightarrow 0$ (alternatively written $\delta \ll \varepsilon$), which yields $\mathcal{P}_{\partial\partial} = -1$. Or we have $\delta \gg \varepsilon$ leading to $\mathcal{P}_{\partial\partial} = +1$. Hence, it is natural to divide \mathcal{K} into two regions via a line $\delta = \kappa\varepsilon$ for a fixed constant $\kappa > 0$. The constant κ is somewhat arbitrary as long as it is independent of ε and δ so we just write for the codimension-one subdivision line $\mathcal{K} \cap \{\varepsilon \simeq \delta\}$; see Figure 4.

3. DOUBLY-SINGULAR SYSTEMS

As a next step, it is important to demonstrate that different classes of doubly-singularly perturbed differential equations fit within and benefit from the more unified view described so far. We shall illustrate this aspect with several very recent examples, where one cannot only recast the problem within our framework but where the main strategy and effects become very transparent as a result.

3.1. Multiple Time Scale Systems

We start with arguably one of the most classical [25, 122, 181] cases of singular perturbation problems [182, 209], namely ordinary differential equations (ODEs) with two time scales, so-called fast-slow systems [128, 131, 145]. A good illustration within this context is to consider the transcritical fast-slow bifurcation normal form

$$\begin{aligned} \frac{dx}{dt} &= x' = (x-y)(x+y) + \frac{\varepsilon^2}{\delta}, \\ \frac{dy}{dt} &= y' = \varepsilon, \end{aligned} \quad (\mathcal{X}_{tc})$$

which is a well-studied system [142]. As before, we shall assume that $\varepsilon \geq 0$ is a small parameter and then consider the case when $\delta \geq 0$ is a second small parameter. Taking the fast subsystem limit (\mathcal{X}_{tc}) given by $\varepsilon \rightarrow 0$ yields

$$\begin{aligned} x' &= x^2 - y^2, \\ y' &= 0, \end{aligned} \quad (\mathcal{A}_{tc,f}^{\varepsilon=0})$$

which is just a standard transcritical bifurcation with the slow variable y acting as a bifurcation parameter. If we re-scale time as $s := \varepsilon t$ and take the singular limit $\varepsilon \rightarrow 0$ again, then one obtains the slow subsystem

$$\begin{aligned} 0 &= (x-y)(x+y), \\ \frac{dy}{ds} &= 1. \end{aligned} \quad (\mathcal{A}_{tc,s}^{\varepsilon=0})$$

The fast and slow subsystems ($\mathcal{A}_{tc,f}^{\varepsilon=0}$)-($\mathcal{A}_{tc,s}^{\varepsilon=0}$) already show a singular structure as the systems are differential equations of different types. The algebraic constraint within the slow subsystem is given by the critical manifold

$$\mathcal{C}_0 := \{(0,0)\} \cup \mathcal{C}_0^{a-} \cup \mathcal{C}_0^{a+} \cup \mathcal{C}_0^{r-} \cup \mathcal{C}_0^{r+}$$

where $\mathcal{C}_0^{a-} := \{|x| = |y|, x < 0, y < 0\}$, $\mathcal{C}_0^{a+} := \{|x| = |y|, x < 0, y > 0\}$, $\mathcal{C}_0^{r-} := \{|x| = |y|, x > 0, y < 0\}$, and $\mathcal{C}_0^{r+} := \{|x| = |y|, x > 0, y > 0\}$ are normally hyperbolic since the linearization with respect to the fast variables yields $D_x(x^2 - y^2) = 2x$, which is nonzero on $\mathcal{C}_0 \setminus \{(0,0)\}$. The critical manifold \mathcal{C}_0 consists of equilibrium points for the fast subsystem; see also Figure 5. Fenichel Theory [88, 128, 145] implies that there exist associated slow manifolds $\mathcal{C}_\varepsilon^{a\pm}$ and $\mathcal{C}_\varepsilon^{r\pm}$.

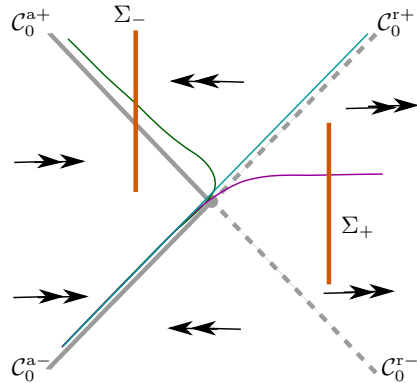


FIG. 5: Sketch of the possible dynamics of (\mathcal{X}_{tc}) in (x, y) -coordinates. The critical manifold \mathcal{C}_0 is shown in gray (repelling parts with dashed lines and attracting parts with solid lines). Three trajectories (green, cyan, magenta) for $0 < \varepsilon \ll 1$ are indicated for three different choices of δ (corresponding to the exchange-of-stability, canard, and critical transition cases respectively). Double arrows show the direction of the fast subsystem flow for orientation; the slow subsystem dynamics on \mathcal{C}_0 is always directed upwards at unit speed.

A generally very important question in many applications is how trajectories of fast-slow systems pass through the region of a transcritical bifurcation of the fast subsystem; for example, there are applications in ecology [51, 135], chemistry [143], numerical analysis [82], epidemiology [124] and network science [125]. Suppose we start with a trajectory $\gamma = \gamma(t)$ at a typical point on the attracting critical manifold \mathcal{C}_0^{a-} , say $\gamma(0) = (x(0), y(0)) = (-3, -3)$ for concreteness as the following arguments do not change up to scaling by fixed constants. By Fenichel Theory, we have that $\gamma(0)$ is $\mathcal{O}(\varepsilon)$ -close to the slow manifold $\mathcal{C}_\varepsilon^{a-}$. We are going to define two one-dimensional sections:

$$\Sigma_- := \{x = -2, y \in [1, 3]\}, \quad \Sigma_+ := \{x = 2, y \in [-1, 1]\}.$$

One may easily prove that the trajectory γ will first get attracted to $\mathcal{C}_\varepsilon^{a-}$ exponentially fast and then track this manifold up towards the origin due to the slow dynamics. Then there are three cases [142]:

- (I) If $\delta(\varepsilon) = \varepsilon(1 + \mathcal{O}(|\varepsilon|^p))$, for some $p > 0$, then the trajectory will intersect Σ_- .
- (II) If $\delta(\varepsilon) = \varepsilon(1 - \mathcal{O}(|\varepsilon|^p))$, for some $p > 0$, then the trajectory will intersect Σ_+ .
- (III) If $\delta(\varepsilon) = \varepsilon(1 \pm \mathcal{O}(\exp(-K/\varepsilon)))$, then the trajectory will never intersect Σ_\pm .

This classification is important as in case (I) we have an exchange-of-stability as γ starts to track the attracting slow manifold $\mathcal{C}_\varepsilon^{a+}$, while in case (II), there is a critical transition leading to a jump near the fast subsystem bifurcation point. In case (III), we have that γ starts to track the repelling branch $\mathcal{C}_\varepsilon^{r+}$ for a slow time of order

$\mathcal{O}(1)$, which means that we have a canard orbit [26, 145]. Hence, since these three cases differ crucially for application purposes, it makes sense to define a property \mathcal{P}_{tcd} by a variable having just three possible values corresponding to the cases (I)–(III) respectively. This provides us with the double singular limit in the cone \mathcal{K} shown in Figure 6.

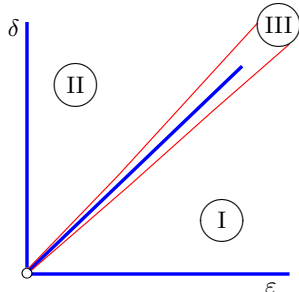


FIG. 6: Classification diagram with respect to the property \mathcal{P}_{tcd} for the problem $(\mathcal{X}_{\text{tc}})$. The three regions correspond to the cases (I)–(III) above yielding exchange-of-stability, critical transition, and canard cases respectively.

In particular, the line $\delta(\varepsilon) = \varepsilon$ becomes a natural dividing line around which we find an asymptotically exponentially small wedge. Outside this wedge, we have two completely different dynamical behaviors (I) and (II) as described above. Note that it also makes sense to formally continue the classification of (I) and (II) onto the two lines $\{\varepsilon = 0, \delta > 0\}$ and $\{\varepsilon > 0, \delta = 0\}$ by using so-called candidate trajectories obtained by concatenating orbits of the suitable fast and slow subsystem singular limit problems. Yet, we evidently cannot make a meaningful classification at the origin $(\varepsilon, \delta) = (0, 0)$ itself regarding our property due to the undefined expression ε^2/δ in the last term of the fast variable dynamics in this case.

Obviously, the fast-slow normal form transcritical bifurcation case we have discussed here is just one of many cases in multiple time scale dynamics where several small parameters appear [145]. Another important system directly motivated by a particular application to the peroxidase-oxidase reaction is the Olsen model [67, 178]. It is given by

$$\begin{aligned} \frac{da}{ds} &= \delta^2(p_1 - \alpha a) - aby, \\ \frac{db}{ds} &= \varepsilon(\delta\varepsilon - \delta bx) - \delta aby, \\ \varepsilon \frac{dx}{ds} &= -x^2 + \varepsilon(b - p_2)x + 3aby + \varepsilon^2 p_4, \\ \frac{dy}{ds} &= p_3(x^2 - y - aby), \end{aligned} \quad (\mathcal{X}_{01})$$

where $(a, b, x, y) \in (\mathbb{R}^+)^4$, we fix the parameters $p_1 = 0.97$, $p_2 = 0.98$, $p_3 = 3.93$, $p_4 = 1.2 \cdot 10^{-5}$ to the classical values considered by Olsen [67, 178] and take ε, δ as the small parameters. Then one can prove [147] that for

$$\varepsilon^2 \ll \delta,$$

the system (\mathcal{X}_{01}) exhibits non-standard, but regularly periodic, relaxation oscillations [172]. A singular limit

geometric phase space description [147], as well as numerical simulations [67, 178] and numerical continuation calculations [69, 174], strongly suggest that there are at least two further important asymptotic regimes namely

$$\varepsilon^2 \gg \delta \quad \text{and} \quad \kappa\varepsilon^2 = \delta = \delta(\varepsilon), \quad \kappa = \mathcal{O}(1),$$

as $\varepsilon \rightarrow 0$. In these cases one observes mixed-mode oscillations (MMOs) [68] and chaotic oscillations respectively, i.e., we have for the Olsen model

(I) $\varepsilon^2 \ll \delta$: non-standard relaxation oscillations,

(II) $\kappa\varepsilon^2 = \delta$: chaotic oscillations,

(III) $\varepsilon^2 \gg \delta$: mixed-mode oscillations,

which is illustrated in Figure 7.

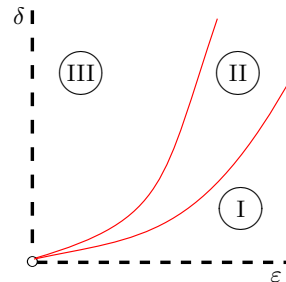


FIG. 7: Classification diagram with respect to the property \mathcal{P}_{osc} for the problem (\mathcal{X}_{01}) . Note that the two parabolic thin curves (red) have the same function form $\delta(\varepsilon) = \kappa\varepsilon^2$ just with two different constants $\kappa > 0$. The three regions correspond to the cases (I)–(III) above yielding non-standard relaxation oscillations, MMOs, and chaotic oscillations respectively.

If we want to distinguish the three different classes of oscillation patterns (relaxation, MMO, chaos), then it does not suffice to rely on natural distinguishing properties individually such as number of maxima for one variable within a time interval \mathcal{P}_{max} , the sign of the top/leading Lyapunov exponent \mathcal{P}_{Lya} , or topological equivalence of the phase portraits \mathcal{P}_{top} . For example, one expects that stable relaxation oscillations and MMOs may have topologically equivalent phase portraits and negative Lyapunov exponents for certain parameters. Furthermore, the number of maxima is also not a good indicator alone as for a given initial condition and a fixed time interval it is easily conceivable that an MMO and a chaotic oscillation have the same \mathcal{P}_{max} . Yet, suppose we fix a generic initial condition in the positive quadrant and a positive sufficiently large fixed time $T = K\varepsilon$ with a constant $K > 0$ such that for \mathcal{P}_{max} we have a fixed number $\mathcal{P}_{\text{max}} = K_0 > 0$ for the case of non-standard relaxation oscillations. Let us define

$$\mathcal{P}_{\text{osc}} := \mathcal{P}_{\text{max}} \mathcal{P}_{\text{Lya}};$$

then we expect that all three cases are different. Indeed, we conjecture that

- $\mathcal{P}_{\text{osc}} = -K_0$: stable non-standard relaxation oscillations;

- $\mathcal{P}_{\text{osc}} < -K_0$: stable mixed-mode oscillations;
- $\mathcal{P}_{\text{osc}} > 0$: chaotic oscillations.

Evidently, this is not a full classification, nor yet rigorously proven beyond the non-standard relaxation case. However, it is very helpful to conceptually understand the Olsen model and its analysis; see Figure 7. The difficulties of the problem are now made precise and much more apparent. Already defining the property \mathcal{P} can be crucial to make the mathematical analysis tractable as proving a precise shape of a trajectory as well as an estimate of the Lyapunov exponent are highly non-trivial for global orbits of non-linear systems. Although methods from geometric singular perturbation theory exist to try to deal with this situation [98], we expect that for the Olsen model these may have to be augmented by computer-assisted proof techniques [101] to actually deal with tracking the dynamics in certain two- and three-dimensional reduced systems. As another question, Figure 7 points us immediately to the transition regimes, i.e., one should ask how trajectories are deformed near the separating asymptotic boundary curves and what happens near/on the non-negative cone $\partial\mathcal{K}$ in (ε, δ) -parameter space. Such a discussion is beyond the scope of this work.

For our examples so far, the second small parameter arose due to the need to study a bifurcation problem, and the bifurcation parameter produced a double singular limit. Yet, in many applications there are additional “physical” modeling constraints, which naturally lead to two small parameters. A typical case is the effect of small noise, which is going to be discussed in the next subsection.

3.2. Stochastic Fast-Slow Systems

Among the most popular models for random noise acting on a dynamical system are stochastic differential equations (SDEs) driven by a Wiener process. There is a broad literature on such equations, based on different approaches such as analysing the Fokker–Planck equation [110], the theory of large deviations [91], and random dynamical systems [2]. Stochastic systems with multiple timescales have been more particularly analysed in [32, 129, 186]. The stochastic dynamics near bifurcation points has been studied, for instance, in [62, 123, 148, 199, 202]. A particularly important field of applications is neuroscience. In this respect, we refer to [205] for an overview, and to [14, 47, 74, 106, 138, 158, 159, 173, 197] for examples of specific problems involving bifurcations.

Consider a stochastic differential equation of the form

$$dx_t = f(x_t, \varepsilon t)dt + \sigma dW_t, \quad (4)$$

where $f : \mathbb{R}^2 \rightarrow \mathbb{R}$ is sufficiently smooth, and W_t is a Wiener process describing white noise. The small parameters are ε , which measures the slow drift of the “parameter” $y = \varepsilon t$, and σ , which measures the noise intensity.

In order to understand the influence of the noise on time scales, let us start by considering the case where $f = f(x)$ does not depend on the second variable, and let V be a potential such that $f(x) = -V'(x)$. Assume that V has a minimum at $x = 0$. Then the theory of large deviations [91] implies that the probability of a solution of the SDE starting from $x_0 = 0$ to reach a point x in a time of order 1 is of order $e^{-V(x)/(2\sigma^2)}$, assuming V is monotonous between 0 and x . This implies the so-called Arrhenius law [4], which states that the expected time for the solution to reach x has order $e^{V(x)/(2\sigma^2)}$. Solutions of the SDE thus tend to spend exponentially long time spans near stable stationary points of f .

When considering the slowly time-dependent system (4), it is convenient to scale time by a factor ε , so that f changes by order 1 in times of order 1. The rescaled system reads

$$dx_t = \frac{1}{\varepsilon} f(x_t, t)dt + \frac{\sigma}{\sqrt{\varepsilon}} dW_t, \quad (\mathcal{X}_{\text{sfs}})$$

where the factor $\sqrt{\varepsilon}$ is due to the scaling property of the Wiener process. Assume f has a smooth stable equilibrium branch $x^*(t)$ acting as a critical manifold for $(\mathcal{X}_{\text{sfs}})$. This means that $f(x^*(t), t) = 0$ for all t in some interval I , and that $a^*(t) = \partial_x f(x^*(t), t)$ is negative, bounded away from 0 in I . In the deterministic case $\sigma = 0$, it is well known [88, 204] that for small ε , $(\mathcal{X}_{\text{sfs}})$ admits a so-called slow solution $\bar{x}(t)$ staying at a distance of order ε from $x^*(t)$.

Let us now fix, say, $I = [0, 1]$, and consider the solution of $(\mathcal{X}_{\text{sfs}})$ starting at time 0 in $\bar{x}(0)$. Denote by $P(\sigma, \varepsilon)$ the probability that the solution leaves a neighborhood of $\bar{x}(t)$ at or before time 1. Then

- (I) on one hand, the large-deviation results just mentioned imply that when σ decreases to 0 for fixed $\varepsilon > 0$, $P(\sigma, \varepsilon)$ converges to 0;
- (II) on the other hand, irreducibility of the Markov process $(x_t)_{t \geq 0}$ implies that when ε decreases to 0 for fixed $\sigma > 0$, $P(\sigma, \varepsilon)$ converges to 1.

Hence, the regimes (I)-(II) naturally induce a property \mathcal{P}_{sfs} , which divides the (ε, σ) -space via the escape probability. The transition between $P(\sigma, \varepsilon)$ close to 0 and close to 1 occurs when ε is of order $e^{-H/(2\sigma^2)}$ for an $H > 0$ depending on the considered neighborhood (Figure 8).

A more precise formulation of the regime $\sigma \searrow 0$ has been given in [29, 32]. Let $\mathcal{B}(h)$ be a family of strips centered in $x^*(t)$, of width $h/\sqrt{2|a(t)|}$, where $a(t) = \partial_x f(\bar{x}(t), t)$ is the linearization of f at the slow solution. These strips act as a kind of “confidence intervals”, in the sense that the probability $P_t(h, \sigma, \varepsilon)$ of leaving $\mathcal{B}(h)$ before time t satisfies

$$P_t(h, \sigma, \varepsilon) \simeq \left[\frac{1}{\varepsilon} \int_0^t |a(s)| ds \right] \frac{h}{\sigma} e^{-h^2/(2\sigma^2)} \quad (5)$$

as long as $t \ll \varepsilon e^{ch^2/\sigma^2}$ for some constant $c > 0$ (see [32, Theorem 3.1.10] for a precise formulation). Choosing h

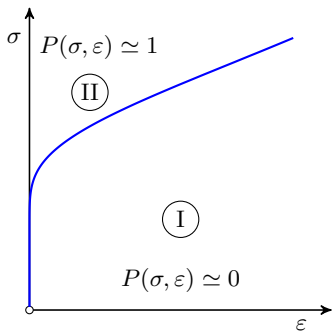


FIG. 8: Probability $P(\sigma, \varepsilon)$ that a solution of the SDE (\mathcal{X}_{sfs}) leaves the neighborhood of a stable critical manifold in slow time of order 1, in the parameter space (ε, σ) . The probability is close to 0 or 1, except near the curve $\varepsilon = \exp[-H/(2\sigma^2)]$.

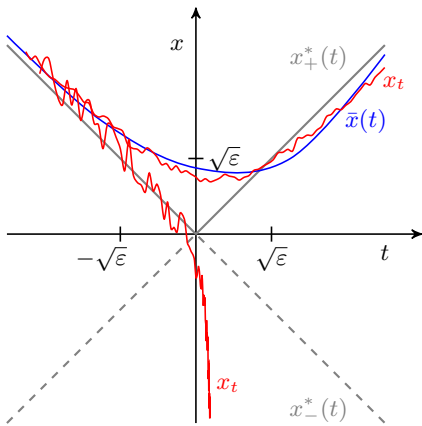


FIG. 9: Slow passage through a transcritical bifurcation. The blue curve is a deterministic solution of (\mathcal{X}_{tcs}) with $\sigma = 0$, which stays at distance at most of order $\sqrt{\varepsilon}$ from the stable critical curve $x^*_+(t) = |t|$. Red paths sketch the behavior of typical stochastic solutions x_t , in parameter regimes (I) (upper path) and (II) (lower path).

of order $\sigma\sqrt{2\log(t/(\varepsilon p))}$, we obtain $P_t(h, \sigma, \varepsilon) \simeq p$, so that $\mathcal{B}(h)$ is indeed a confidence strip at level p .

This first example of a two-scale behavior for an SDE is somewhat atypical compared to other examples given in this review, in the sense that the transition between qualitatively different regimes occurs when ε is exponentially small in σ . Of course, one can “regularize” things by writing $\varepsilon = e^{-\lambda/\sigma^2}$ and describing the behavior in terms of λ and σ . This is the approach adopted in [90] for instance.

More standard examples of double limits can however be found in the vicinity of bifurcation points. Consider for instance the fast-slow SDE (\mathcal{X}_{sfs})

$$dx_t = \frac{1}{\varepsilon}(t^2 - x_t^2)dt + \frac{\sigma}{\sqrt{\varepsilon}}dW_t, \quad (\mathcal{X}_{\text{tcs}})$$

which is a stochastic version of (\mathcal{X}_{tc}). The critical manifold of the deterministic equation $\varepsilon\dot{x} = t^2 - x^2$ is composed of a stable branch $\{x = x^*_+(t) = |t|; t \neq 0\}$ and

an unstable branch $\{x = x^*_-(t) = -|t|; t \neq 0\}$. It is well-known (see for instance [100]) that when $\sigma = 0$, the equation (\mathcal{X}_{tcs}) admits a slow solution $\bar{x}(t)$ of order $\max\{|t|, \sqrt{\varepsilon}\}$. This solution tracks the stable branch $x^*_+(t)$ at a distance of order $\varepsilon/\max\{|t|, \sqrt{\varepsilon}\}$ (Figure 9).

In the case $\sigma > 0$, we can define as above a strip $\mathcal{B}(h)$ centered in the slow solution $\bar{x}(t)$, and of width $h/\sqrt{2|a(t)|}$. Note that this time, the linearization $|a(t)|$ has order $\max\{|t|, \sqrt{\varepsilon}\}$. The width of $\mathcal{B}(h)$ is maximal near $t = 0$, where it has order $h/\varepsilon^{1/4}$. It turns out that one then has two qualitatively different situations [30]:

- (I) If $\sigma \ll \varepsilon^{3/4}$, we can take h of order $\varepsilon^{3/4}$ and still have a strip $\mathcal{B}(h)$ staying away from the origin. One can then show that the probability of a solution of (\mathcal{X}_{tcs}) leaving $\mathcal{B}(h)$ before, say, time 1, has order $\exp[-h^2/(2\sigma^2)] = \exp[-\varepsilon^{3/2}/\sigma^2]$, which is exponentially small in this regime.
- (II) If $\sigma \gg \varepsilon^{3/4}$, on the other hand, any strip $\mathcal{B}(h)$ with $h \geq \sigma$ intersects the t -axis already at or before a time of order $-\sigma^{2/3}$. One can then show that it is very likely that the solution x_t becomes negative, of order 1, shortly after time $-\sigma^{2/3}$. The probability that x_t remains positive up to time 1 has order $e^{-\sigma^{4/3}/(\varepsilon \log(\sigma^{-1}))}$.

One can summarize the difference between the two regimes by considering the transition probability

$$P_{\text{trans}}(\sigma, \varepsilon) = \mathbb{P}^{(\bar{x}(t_0), t_0)}\{\exists t \leq 1: x_t = -1\}, \quad (6)$$

where the superscript $(\bar{x}(t_0), t_0)$ indicates the initial condition. For negative t_0 of order 1, we have

$$P_{\text{trans}}(\sigma, \varepsilon) \begin{cases} \leq e^{-\kappa\varepsilon^{3/2}/\sigma^2} & \text{in Regime (I) ,} \\ \geq 1 - e^{-\kappa\sigma^{4/3}/(\varepsilon \log(\sigma^{-1}))} & \text{in Regime (II) ,} \end{cases} \quad (7)$$

for a constant $\kappa > 0$ (Figure 10). Hence, we can again use a suitable transition probability to define a property \mathcal{P}_{tcs} , which provides at least two clearly distinct asymptotic regimes (I)-(II) in the double limit. See [32, Theorems 3.5.1 and 3.5.2] for precise formulations of these results.

An interesting generalization of Example (\mathcal{X}_{tcs}) is the SDE

$$dx_t = \frac{1}{\varepsilon}(t^2 - x_t^2 + \delta)dt + \frac{\sigma}{\sqrt{\varepsilon}}dW_t, \quad (\mathcal{X}_{\text{tcd}})$$

where the parameter $\delta > 0$ plays the same role as ε/δ in (\mathcal{X}_{tc}). Note that we are now dealing with three small parameters ε , σ , and δ . The critical manifolds are given here by $x^*_\pm(t) = \pm\sqrt{t^2 + \delta}$, so that they do not quite touch: their minimal distance is $2\sqrt{\delta}$.

A similar analysis as for the transcritical bifurcation (\mathcal{X}_{tcs}) can be made, and results in the following case distinction (Figure 11, see [30, Theorems 2.6 and 2.7] for precise formulations):

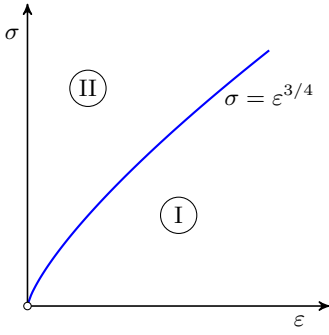


FIG. 10: The probability P_{trans} that the solutions x_t of equation (\mathcal{X}_{tcs}) starting on the stable slow solution $\bar{x}(t)$ becomes negative behaves differently in the two shown parameter regions. In Region (I), P_{trans} has order $\exp[-\varepsilon^{3/2}/\sigma^2]$, while in Region (II), $1 - P_{\text{trans}}$ has order $\exp[-\sigma^{4/3}/(\varepsilon \log(\sigma^{-1}))]$.

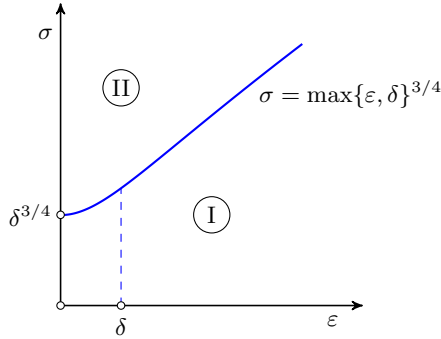


FIG. 11: (ε, σ) -parameter plane for the SDE (\mathcal{X}_{tca}) describing an avoided transcritical bifurcation, for a fixed $\delta > 0$. In Region (I), the transition probability P_{trans} has order $\exp[-\max\{\varepsilon, \delta\}^{3/2}/\sigma^2]$, while in Region (II), $1 - P_{\text{trans}}$ has order $\exp[-\sigma^{4/3}/(\varepsilon \log(\sigma^{-1}))]$.

- (I) If $\sigma \ll \max\{\varepsilon, \delta\}^{3/4}$, solutions tend to stay near the slow solution $\bar{x}(t)$ tracking $x_+^*(t)$, and the transition probability P_{trans} is exponentially small.
- (II) If $\sigma \gg \max\{\varepsilon, \delta\}^{3/4}$, solutions are likely to escape to negative values of x as soon as t is slightly larger than $-\sigma^{2/3}$.

This results in a transition probability behaving as

$$P_{\text{trans}}(\sigma, \varepsilon) \begin{cases} \leq e^{-\kappa \max\{\varepsilon, \delta\}^{3/2}/\sigma^2} & \text{in Regime (I) ,} \\ \geq 1 - e^{-\kappa \sigma^{4/3}/(\varepsilon \log(\sigma^{-1}))} & \text{in Regime (II) .} \end{cases} \quad (8)$$

The parameter δ thus causes a saturation effect at small values of ε .

The examples considered so far were all particular cases of the slowly time-dependent SDE (\mathcal{X}_{sfs}). Other types of bifurcations, such as the saddle-node bifurcation, which results in similar regimes with different exponents, are described in [32, Chapter 3]. One can however also

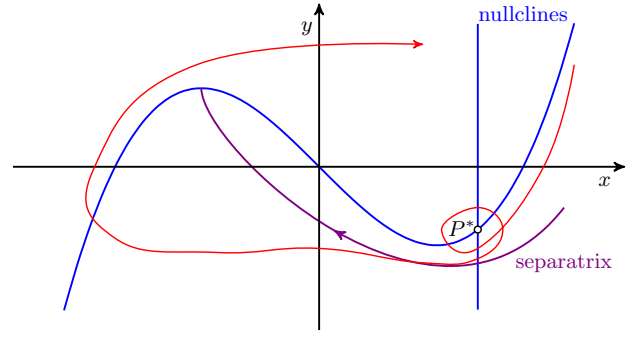


FIG. 12: Phase space of the stochastic FitzHugh–Nagumo system (\mathcal{X}_{FHS}). The separatrix is defined as the deterministic negative orbit of the local maximum of the x -nullcline $\{y = x^3 - x\}$. When P^* is a focus, stochastic solutions tend to perform small oscillations around P^* before crossing the separatrix, and making a large excursion (or spike) before returning near P^* .

consider fully coupled fast-slow systems of the form

$$\begin{aligned} dx_t &= \frac{1}{\varepsilon} f(x_t, y_t) dt + \frac{\sigma}{\sqrt{\varepsilon}} F(x_t, y_t) dW_t, \\ dy_t &= g(x_t, y_t) dt + \sigma' G(x_t, y_t) dW_t, \end{aligned} \quad (9)$$

where $x \in \mathbb{R}^m$, $y \in \mathbb{R}^n$, and W_t is a k -dimensional Wiener process. In a similar way as for (4), one can obtain concentration results for solutions near stable normally hyperbolic critical manifolds, see [31].

A particularly interesting case is the stochastic FitzHugh–Nagumo system modelling action potential dynamics of individual neurons, investigated in [35, 173]. We consider here the particular case

$$\begin{aligned} dx_t &= \frac{1}{\varepsilon} [x_t - x_t^3 + y_t] dt + \frac{\sigma}{\sqrt{\varepsilon}} dW_t^{(1)}, \\ dy_t &= [a - x_t] dt + \sigma dW_t^{(2)}, \end{aligned} \quad (\mathcal{X}_{\text{FHS}})$$

where $W_t^{(1)}$ and $W_t^{(2)}$ are independent Wiener processes. In the deterministic case $\sigma = 0$, the system (\mathcal{X}_{FHS}) has a unique equilibrium point $P^* = (a, a^3 - a)$. The eigenvalues of the linearisation at P^* are given by

$$\lambda_{\pm} = \frac{-\delta \pm \sqrt{\delta^2 - \varepsilon}}{\varepsilon}, \quad \delta = \frac{3a^2 - 1}{2}. \quad (10)$$

Hence P^* is a stable node for $\delta > \sqrt{\varepsilon}$, a stable focus for $0 < \delta < \sqrt{\varepsilon}$, an unstable focus for $-\sqrt{\varepsilon} < \delta < 0$, and an unstable node for $\delta < -\sqrt{\varepsilon}$.

We are interested here in the excitable regime $0 < \delta \ll 1$, $\sigma > 0$. In that situation, though P^* is stable in the deterministic case, it lies close to a (pseudo-)separatrix (Figure 12). Whenever the noise kicks it over the separatrix, the system makes a large excursion before returning to its rest state, producing a so-called *spike* of the neuron's membrane potential.

In [173], the authors investigated the stochastic system (\mathcal{X}_{FHS}) via formal computations, and found a large

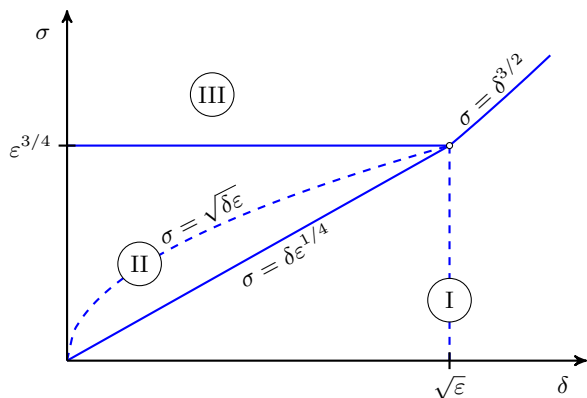


FIG. 13: (δ, σ) -parameter plane for the stochastic FitzHugh–Nagumo SDE (\mathcal{X}_{FHS}), for a fixed $\varepsilon > 0$. The three regions correspond to (I) rare isolated spikes, (II) clusters of spikes, and (III) repeated spikes.

number of different parameter regimes. Some of these formal results have been proved rigorously in [35]. One can identify three main parameter regimes, as shown in Figure 13:

- (I) If $0 < \delta < \sqrt{\varepsilon}$ and $\sigma \ll \delta\varepsilon^{1/4}$ or if $\sqrt{\varepsilon} \leq \delta \ll 1$ and $\sigma \ll \delta^{3/2}$, the system displays rare isolated spikes (Figure 14-(I)). In particular, [35, Theorem 3.2] shows that if $\delta/\sqrt{\varepsilon}$ is sufficiently small, then the expected number of small oscillations around P^* between two consecutive spikes has order $\exp\{\delta^2\sqrt{\varepsilon}/\sigma^2\}$.
- (II) If $0 < \delta < \sqrt{\varepsilon}$ and $\delta\varepsilon^{1/4} \leq \sigma \leq \varepsilon^{3/4}$, one can observe clusters of spikes (Figure 14-(II)). In fact, what happens is that as σ increases, the probability that a spike is immediately followed by another spike gradually increases like

$$\Phi\left(-\frac{\varepsilon^{1/4}(\delta - \sigma^2/\varepsilon)}{\sigma}\right), \quad (11)$$

where Φ denotes the distribution function of a standard normal random variable. The dashed curve $\sigma = \sqrt{\delta\varepsilon}$ in Figure 13 corresponds to this probability being close to 1/2 (see [35, Section 5]).

- (III) If $0 < \delta < \sqrt{\varepsilon}$ and $\sigma \gg \varepsilon^{3/4}$ or if $\sqrt{\varepsilon} \leq \delta \ll 1$ and $\sigma \gg \delta^{3/2}$, the system displays repeated spikes (Figure 14-(III)), meaning that after having spiked, it is very likely to spike again immediately.

Note that these three regimes actually use a probabilistic asymptotic spiking pattern to define a property \mathcal{P}_{FHS} to dissect the (triple) singular limit parameter space. So the example nicely illustrates that also on a stochastic level, one can use macroscopic patterns, and that quite frequently even more than two small parameters are relevant.

The behavior in regimes just described in (I)–(III) can be considered as a stochastic instance of mixed-mode oscillations (MMOs) [68], in which small-amplitude and

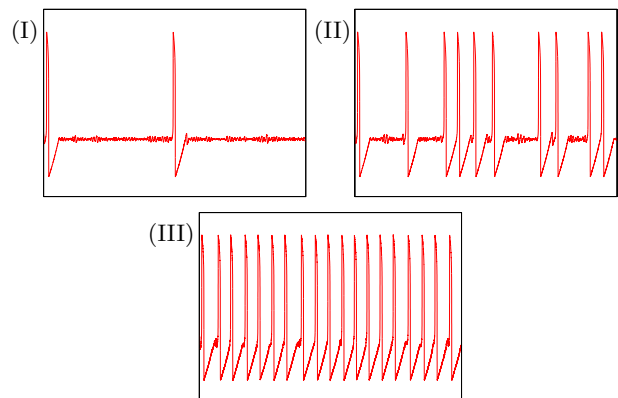


FIG. 14: Time series $-x_t$ of solutions to the stochastic FitzHugh–Nagumo equation (\mathcal{X}_{FHS}) in three different parameter regimes. Parameter values are $\varepsilon = 0.01$, $\delta = 0.03$, and (I) $\sigma = 0.001$, (II) $\sigma = 0.0025$ and (III) $\sigma = 0.01$.

large-amplitude oscillations alternate; cf. problem (\mathcal{X}_{O1}). While deterministic MMOs often show a regular pattern, and sometimes a chaotic pattern, in the stochastic case considered here the number of small and large-amplitude oscillations are random variables. More intricate patterns can arise near folded-node bifurcations in three-dimensional SDEs, as for instance in the Koper model [33, 34].

The examples in this subsection have shown that the interplay between a deterministic multiple time scale system with small noise provides a very natural class of systems, and small noise induces a doubly singularly perturbed problem. Yet, stochastic differential equations provide many other natural avenues to double limits, even without explicit time scale separation for the drift. This is illustrated by the next subsection.

3.3. Shear-Induced Chaos

In this section, we consider the interaction of shear forces and stochastic noise that can generate a switching from synchronization to chaotic behavior in stochastic oscillators. The onset of chaos by an interplay of shear and, typically small, noise has been broadly discussed within the context of stochastic Hopf bifurcation [3, 15–17, 75, 156, 194], with important connections to coupled (neural) oscillators [42, 155, 157, 215] and questions around the role of noise and chaos in (turbulent) fluid flows [1, 87, 111, 112]. Note that the idea of adding small noise to prove chaotic properties in the deterministic zero-noise limit has become an important tool in dynamical systems theory in recent years [43, 44, 81, 218].

As a basic toy model (cf. [83]), we consider the SDE, written in Stratonovich form,

$$\begin{aligned} dy &= -\alpha y dt + \sigma \sum_{i=1}^m f_i(\vartheta) \circ dW_t^i, \\ d\vartheta &= (1 + by) dt, \end{aligned} \quad (\mathcal{X}_{\text{sic}})$$

where $(y, \vartheta) \in \mathbb{R} \times \mathbb{S}^1$ are cylindrical amplitude-phase coordinates, $m \geq 1$ is a natural number, and W_t^i for $i \in \{1, \dots, m\}$ denote independent one-dimensional Brownian motions. We will assume that $\alpha, \sigma, b \geq 0$, i.e. all parameters are non-negative.

When there is no noise ($\sigma = 0$), the ODE (\mathcal{X}_{sic}) has a globally attracting limit cycle at $y = 0$ with contraction rate $\alpha > 0$; for $\alpha = 0$, every trajectory is a periodic orbit at some $y \in \mathbb{R}$. In the presence of noise ($\sigma > 0$), the amplitude direction is driven by phase-dependent random perturbations. The real parameter b induces an effect which is often called shear: if $b > 0$, the phase velocity depends on the amplitude y .

In the tradition of random dynamical systems theory [2], and in contrast to the sample paths approach in the last subsection, we now compare trajectories with different initial conditions but driven by the same noise. As trajectories depend on the noise realization, one cannot expect any convergent behavior of individual trajectories to a fixed attractor. An alternative point of view avoiding this problem is to consider, for a fixed noise realization in the past, the flow of a set of initial conditions from time $t = -T$ to a fixed endpoint in time, say $t = 0$, and then take the (pullback) limit $T \rightarrow \infty$. If trajectories of initial conditions converge under this procedure to some set, then this set is called a random pullback attractor, or simply random attractor.

Typically, one can observe two different scenarios generated by the impact of noise on a stable limit cycle, as in model (\mathcal{X}_{sic}) with $\alpha > 0$: either synchronization of trajectories towards a random equilibrium (see Figure 15 (a)-(c)), or separation of trajectories within an attracting object, a random strange attractor with fractal properties (see Figure 15(d)-(f)). The crucial quantity for determining the character of the dynamics is the sign of the first Lyapunov exponent $\lambda_1 = \lambda_1(\alpha, b, \sigma)$ with respect to the ergodic invariant measure of the random system. The quantity λ_1 can be summarized as the dominant infinitesimal asymptotic growth rate of almost all trajectories.

The mechanism, whereby a combination of shear and noise leads to a positive Lyapunov exponent, was described as shear-induced chaos [156]. The noise perturbations drive some points of the deterministic limit cycle up and some down on the cylinder. Due to the phase-amplitude coupling b , the points with larger y -coordinates move faster in the ϑ -direction. At the same time, the dissipation force with strength α attracts the curve back to the limit cycles. This provides a mechanism for stretching and folding characteristic of chaos. The transition to chaos in the continuous time stochastic forcing is much faster than in the case of, e.g., periodic kicks [156]. This is due to the fact that points end up in areas with arbitrarily large values of y with positive probability such that already small shear can generate the described stretching and folding.

The validity of this mechanism has first been demonstrated analytically [185, 211, 212] in the case of periodically kicked limit cycles, including probabilistic charac-

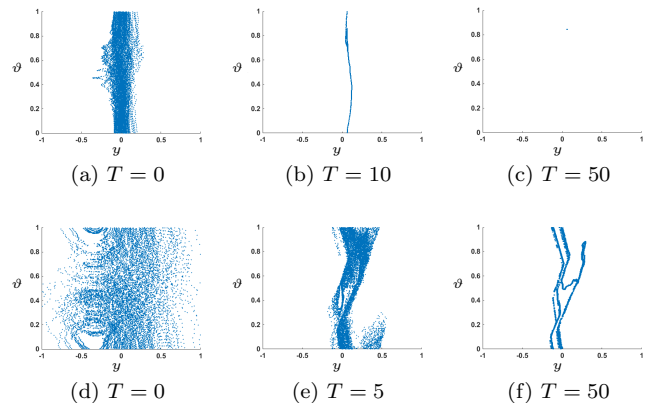


FIG. 15: Pullback attraction to random equilibrium (a)-(c) for model (\mathcal{X}_{sic}) with $\sigma = 0.5, \alpha = 1.5, b = 3$ such that $\lambda_1 < 0$, and to random strange attractor (d)-(f) for $\sigma = 2, \alpha = 1.5, b = 3$ such that $\lambda_1 > 0$.

terizations of the dynamics. An analytical proof of shear-induced chaos in the stochastic setting was developed in [83]. Based on a specific machinery to explicitly express Lyapunov exponents for noisy oscillators [117, 118] one can provide the formula

$$\lambda_1(\alpha, b, \sigma) = -\frac{\alpha}{2} + \frac{b\sigma}{2} \int_0^\infty v m_{\sigma, b, \alpha}(v) dv, \quad (12)$$

$$\lambda_2(\alpha, b, \sigma) = -\frac{\alpha}{2} - \frac{b\sigma}{2} \int_0^\infty v m_{\sigma, b, \alpha}(v) dv, \quad (13)$$

where

$$m_{\sigma, b, \alpha}(v) = \frac{\frac{1}{\sqrt{v}} \exp\left(-\frac{b\sigma}{6}v^3 + \frac{\alpha^2}{2b\sigma}v\right)}{\int_0^\infty \frac{1}{\sqrt{u}} \exp\left(-\frac{b\sigma}{6}u^3 + \frac{\alpha^2}{2b\sigma}u\right) du}, \quad (14)$$

and λ_2 is the second Lyapunov exponent, which is always negative unless $\alpha = \sigma = 0$. Furthermore, one can prove the following result [83]: assume the functions $f_i : \mathbb{S}^1 \simeq [0, 1) \rightarrow \mathbb{R}$ to be $C^{2, \kappa}$ for some $0 < \kappa \leq 1$ to guarantee differentiability of the random dynamical system (see [2, Theorem 2.3.32]), and, to make explicit calculations possible, assume $m \geq 2$ with

$$\sum_{i=1}^m f_i'(\vartheta)^2 = 1 \quad \text{for all } \vartheta \in \mathbb{S}^1. \quad (15)$$

Then there is $c_0 \approx 0.2823$ such that for all $\alpha, b > 0$, the number

$$\sigma_0(\alpha, b) = \frac{\alpha^{3/2}}{c_0^{1/2} b} > 0, \quad (16)$$

is the unique value of σ where the top Lyapunov exponent $\lambda_1(\alpha, b, \sigma)$ of (\mathcal{X}_{sic}) changes sign:

$$\lambda_1(\alpha, b, \sigma) \begin{cases} < 0 & \text{if } 0 < \sigma < \sigma_0(\alpha, b), \\ = 0 & \text{if } \sigma = \sigma_0(\alpha, b), \\ > 0 & \text{if } \sigma > \sigma_0(\alpha, b). \end{cases}$$

In particular, we can just use the sign of the top Lyapunov exponent as a natural definition of a property \mathcal{P}_{sic} for the shear-induced chaos problem (\mathcal{X}_{sic}). Figure 16 shows the graph of σ_0 for $0 \leq \alpha \leq 1$ and fixed $b = 1$. Note that for $b, \sigma \neq 0$, we can always conduct a change of variables in the amplitude variable y to rescale the shear parameter b to 1 and the effective noise amplitude to σb . Hence, the above result and the corresponding illustration in Figure 16 hold in precisely the same way, when the roles of σ and b are exchanged.

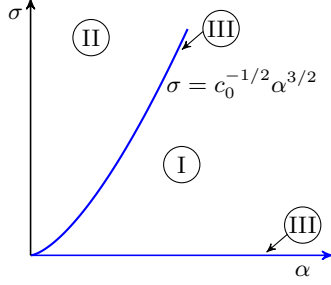


FIG. 16: Fixing $b = 1$ in model (\mathcal{X}_{sic}), the figure shows the areas of negative (I) and positive (II) λ_1 in the (α, σ) -parameter space being separated by the curve $\{(\alpha, \sigma_0(\alpha, 1))\}$ (III) of λ_1 being zero, using formula (16) for σ_0 .

For all fixed $\alpha > 0$, if $\sigma = 0$, i.e., in the zero-noise limit, we clearly have $\lambda_1 = 0$, now seen as the leading Lyapunov exponent associated with the attracting deterministic limit cycle. The convergence can also be seen by a different form of formula (12), which is obtained by a change of variables as

$$\lambda_1(\alpha, b, \sigma) = \frac{\alpha}{2} \left(\int_0^\infty u \tilde{m}_{\sigma, b, \alpha}(u) du - 1 \right), \quad (17)$$

where

$$\tilde{m}_{\sigma, b, \alpha}(u) = \frac{\frac{1}{\sqrt{u}} \exp\left(-\frac{\alpha^3}{\sigma^2 b^2} \left[\frac{1}{6}u^3 - \frac{1}{2}u\right]\right)}{\int_0^\infty \frac{1}{\sqrt{w}} \exp\left(-\frac{\alpha^3}{\sigma^2 b^2} \left[\frac{1}{6}w^3 - \frac{1}{2}w\right]\right) dw}.$$

Hence, there is a continuous transition back to situation (III) at the α -axis. When $\alpha = 0$ but $\sigma > 0$, dissipativity and the existence of a random attractor are lost and the system becomes volume-preserving. Still, the associated first Lyapunov exponent λ_1 is positive and the σ -axis belongs to situation (II), as can be easily seen from formula (12). The origin $(\sigma, \alpha) = (0, 0)$ itself belongs to (III). This gives a full categorization of model (\mathcal{X}_{sic}) in terms of the first Lyapunov exponent under the double limit of the parameters σ, b on the one side and α on the other.

Generally, shear-induced chaos can take more complicated forms with more nonlinearities. A paradigm problem is the normal form of a Hopf bifurcation with additive noise

$$\begin{aligned} dx &= (\alpha x - \beta y - (ax - by)(x^2 + y^2)) dt + \sigma dW_t^1, \\ dy &= (\alpha y + \beta x - (bx + ay)(x^2 + y^2)) dt + \sigma dW_t^2, \end{aligned} \quad (\mathcal{X}_{\text{sH}})$$

where $\sigma \geq 0$ is the strength of the noise, $\alpha \in \mathbb{R}$ equals the real part of eigenvalues of the linearization of the vector field at $(0, 0)$, $b \in \mathbb{R}$ represents shear strength, $\beta \in \mathbb{R}$ is the linear component of rotational speed and W_t^1, W_t^2 denote independent one-dimensional Brownian motions. For $\alpha > 0$, the deterministic system ($\sigma = 0$) possesses a limit cycle at radius $\sqrt{\alpha}/a$, for any fixed $a > 0$, with linear contraction rate -2α .

The model has been studied in [72, 75, 216] with various, predominantly numerical, approaches to describing shear-induced chaos. Hence, it again makes sense to define \mathcal{P}_{sH} via the sign of the first Lyapunov exponent. For (\mathcal{X}_{sH}), only the case of synchronization, i.e. $\lambda_1 < 0$, has been proven analytically [75]. The change of sign of λ_1 to positive values is only proven in the particular context of the conditioned Lyapunov exponent [84], considering the random dynamics on a bounded domain with killing at the boundary, by conducting a computer-assisted proof [52]. An explicit formula as before seems out of scope for system (\mathcal{X}_{sH}) on the whole domain.

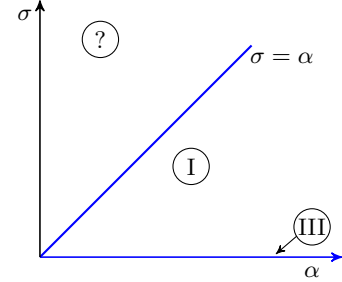


FIG. 17: Fixing all other parameters in model (\mathcal{X}_{sH}), in particular $b \gg \sqrt{2}a$, we consider the (α, σ) -parameter space for α, σ sufficiently small, and can associate the area beneath the diagonal with negative λ_1 (I) and the α -axis, including the origin, with $\lambda_1 = 0$ (III).

However, there are two small parameter results that give some indication concerning the question of double limits in this case and demonstrate the differences to the cylinder model. Firstly, it was shown in [72] and then further elaborated in [75] that for any fixed $a > 0$, $b < \sqrt{2}a$ and α smaller than a given bound depending on all other parameters, the first Lyapunov exponent is negative, i.e. $\lambda_1 < 0$. This means that for the case $b, \alpha \rightarrow 0$ we will always be in scenario (I), in contrast to model (\mathcal{X}_{sic}) where scenario (II) can happen in the double-limiting case, as illustrated in Figure 16 — recall that σ and b are interchangeable in this case and the same formula and corresponding figure are also true for replacing σ by b . This does not transfer to the more complicated, highly nonlinear situation of model (\mathcal{X}_{sH}). Secondly, Deville et al. [72] demonstrate that $\lambda_1 < 0$ for $\sigma \frac{a}{\alpha} \rightarrow 0$. This allows us to give at least a partial picture of the small parameter situation for α, σ when the shear strength $b \gg \sqrt{2}a$ is large; Figure 17 depicts such a sufficiently small domain in parameter space. Analytical approximation of other areas than the one beneath the

diagonal seems out of reach with current methods.

The examples involving SDEs have shown clearly that small noise is a natural source of double limits. Yet, SDEs still carry some regularity due to the (almost $1/2$ -Hölder) continuous input. The next subsection illustrates that even for stochastic switching problems one can frequently identify natural double limits.

3.4. Piecewise Deterministic Processes

Piecewise deterministic processes are stochastic processes that evolve deterministically on most time intervals of short length; random events occur instantaneously and come for example in the shape of random switches between several driving vector fields, or jumps to randomly chosen sites of the phase space. In this subsection, we will consider two instances of piecewise deterministic processes, which are induced by a parameter-dependent differential equation with an intermittently-acting noise that depends itself on a small parameter. We work within the following basic framework: Let M be an open subset of \mathbb{R}^m , $m \in \mathbb{N}$, and let u_0 and u_1 be smooth vector fields on M that depend on a small positive parameter δ . In addition, assume that for $i \in \{0, 1\}$ and for every $x_0 \in M$, the initial-value problem

$$\begin{aligned} \dot{x}(t) &= u_i(x(t)), \quad t > 0, \\ x(0) &= x_0 \end{aligned}$$

has a unique solution $x(t) = \Phi_i^t(x_0)$ that is defined for all $t \geq 0$. Consider the differential equation

$$\frac{dx}{dt} = U(\omega, x(t), t), \quad (\mathcal{X}_{pd})$$

where ω is a realization of a continuous-time Markov chain on $\{0, 1\}$ with transition rates

$$\lambda_0 = \lim_{t \downarrow 0} \frac{\mathbb{P}(\omega_t = 1 | \omega_0 = 0)}{t}, \quad \lambda_1 = \lim_{t \downarrow 0} \frac{\mathbb{P}(\omega_t = 0 | \omega_0 = 1)}{t},$$

and where

$$U(\omega, x, t) := \begin{cases} u_0(x), & \omega_t = 0, \\ u_1(x), & \omega_t = 1. \end{cases}$$

The differential equation in (\mathcal{X}_{pd}) is thus alternately driven by the vector fields u_0 and u_1 , and switches between these vector fields correspond to the jumps of a continuous-time Markov chain. The latter being the only source of randomness, it is natural to assume that the transition rates λ_0 and λ_1 depend on a second small parameter $\varepsilon > 0$. For a typical choice of ω , the equation in (\mathcal{X}_{pd}) has a unique solution $X(\omega)$ that is defined for all $t \geq 0$. The resulting stochastic process $X = (X_t)_{t \geq 0}$ on M can be turned into a Markov process by adjoining the process $E = (E_t)_{t \geq 0}$ on $\{0, 1\}$ defined by $E_t(\omega) := \omega_t$. The resulting two-component process (X, E) on the state

space $M \times \{0, 1\}$ belongs to the class of piecewise deterministic Markov processes [66].

In line with standard terminology, a stationary distribution for (X, E) is a probability measure μ on $M \times \{0, 1\}$ such that for every Borel set $A \subset M$, $i \in \{0, 1\}$, and $t \geq 0$,

$$\mu(A \times \{i\}) = \sum_{j \in \{0, 1\}} \int_M \mathfrak{P}^t(x, j; A \times \{i\}) \mu(dx \times \{j\}),$$

where $(\mathfrak{P}^t)_{t \geq 0}$ denotes the Markov semigroup of (X, E) .

Consider the dynamical system induced by randomly switching between the two-dimensional linear vector fields $u_i(x) = U_i x$, $i \in \{0, 1\}$, where

$$U_0 := \begin{pmatrix} -\delta & 1 \\ 0 & -\delta \end{pmatrix}, \quad U_1 := \begin{pmatrix} -\delta & 0 \\ -1 & -\delta \end{pmatrix}. \quad (\mathcal{X}_{pdl})$$

The switching rates are assumed to be $\lambda_0 = \lambda_1 = \varepsilon^{-1}$, i.e. for small ε we are in the regime of fast switching. This system belongs to the class of switching systems studied in [149]. Here, we present some of the main findings from [149] using the viewpoint of double limits in ε and δ .

Both U_0 and U_1 are defective matrices, meaning that the eigenspaces corresponding to their only eigenvalue $-\delta$ have dimension 1. Since $-\delta < 0$, the equilibrium point $(0, 0)$ shared by u_0 and u_1 is globally asymptotically stable for each individual ODE $\dot{x}(t) = u_i(x(t))$. However, as pointed out in [19], [149] for the random case, and in [12] for the deterministic case, switching between stable ODEs may cause instability. This phenomenon can be easily apprehended if switching takes place between two stable vector fields that admit an unstable average. As the switching rates tend to infinity, the random dynamics start to resemble the deterministic dynamics governed by the unstable average [86]. For the present system, however, the mechanism causing instability is more subtle (Figure 18).

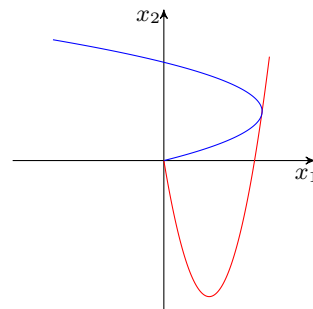


FIG. 18: Sample trajectories for the vector fields u_0 and u_1 associated with (\mathcal{X}_{pdl}) . The blue and red curves represent trajectories for u_0 and u_1 , respectively. If one first flows along the blue curve towards the origin and then switches to the red one at the point where the curves touch, one can increase the distance to the origin.

Let us be more precise: We call the random dynamical system under consideration stable if the stochastic process X on \mathbb{R}^2 , induced by alternately flowing along u_0 and u_1 , satisfies

$$\mathbb{P}_{x,i} \left(\lim_{t \rightarrow \infty} \|X_t\| = 0 \right) = 1$$

for every $x \in \mathbb{R}^2$ and $i \in \{0, 1\}$. Here, $\mathbb{P}_{x,i}$ denotes the law of the Markov process (X, E) starting at (x, i) , and $\|\cdot\|$ is the Euclidean norm on \mathbb{R}^2 . The random dynamical system is said to be unstable if for every $x \in \mathbb{R}^2 \setminus \{(0, 0)\}$ and $i \in \{0, 1\}$,

$$\mathbb{P}_{x,i} \left(\lim_{t \rightarrow \infty} \|X_t\| = \infty \right) = 1.$$

A priori, there may be choices of ε and δ for which the system is neither stable nor unstable. As we are about to see, this is, at least generically, not the case. We want to study the property

$$\mathcal{P}_{\text{pdl}} = \begin{cases} 1 & \text{if the system is stable,} \\ 0 & \text{if the system is unstable.} \end{cases}$$

It is convenient to represent the stochastic process X in polar coordinates (see [134] on the utility of polar decomposition for the study of Lyapunov exponents). Following [19], one defines the radial process $R_t := \|X_t\|$ and the angular process $A_t := X_t / \|X_t\|$ whenever $X_t \neq (0, 0)$. The two-component process (A, E) on $S^1 \times \{0, 1\}$ is then again a piecewise deterministic Markov process characterized by random switching between the vector fields $\theta \mapsto \sin^2(\theta)$ and $\theta \mapsto \cos^2(\theta)$, where S^1 is identified with the interval $[0, 2\pi)$. According to [149, Lemma 3.2], (A, E) admits a unique stationary distribution μ that is absolutely continuous with respect to the product of arc-length measure on S^1 and counting measure on $\{0, 1\}$. In our example, μ only depends on the switching rate, i.e. it is a function of ε while being independent of δ . Let ρ be the probability density function of μ and let $\rho_i(\cdot) := \rho(\cdot, i)$ for $i \in \{0, 1\}$. Since μ is ε -dependent, so are ρ_0 and ρ_1 . Define

$$G(\varepsilon) := \int_0^{2\pi} (\rho_0(\theta) - \rho_1(\theta)) \cos(\theta) \sin(\theta) \, d\theta, \quad (18)$$

which is set up in such a way that the integrand is positive for all $\theta \in [0, 2\pi)$, and thus $G > 0$. From [149, Lemma 3.3] one obtains the following cases:

- (I) If $\delta < G(\varepsilon)$, then $\mathcal{P}_{\text{pdl}} = 0$.
- (II) If $\delta > G(\varepsilon)$, then $\mathcal{P}_{\text{pdl}} = 1$.

There are explicit formulae for ρ_0 and ρ_1 [149]. Together with (18), this yields a reasonably explicit representation for the threshold function G that is in principle amenable to asymptotic analysis.

If $\delta = 0$, $\varepsilon > 0$, the process X alternately moves along lines parallel to the x -axis and lines parallel to the y -axis.

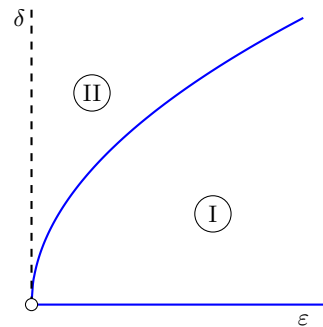


FIG. 19: Classification diagram with respect to the property \mathcal{P}_{pdl} . The two regions (I) and (II) correspond to the cases (I) (stable) and (II) (unstable). The blue curve separating the regions (I) and (II) represents the graph of G . On the δ -axis, the problem is not well-defined, which makes a classification impossible.

It is not hard to see that [149, Lemma 3.3] remains valid in this limiting case. Since $G(\varepsilon) > 0$, one has $\mathcal{P}_{\text{pdl}} = 0$.

If $\varepsilon = 0$, the process X is not well-defined because the switching rates are infinite. It does, however, make sense to study the limiting behavior of the random dynamical system as $\varepsilon \rightarrow 0$. According to [149, Thm. 2.5], for ε sufficiently small (with the required smallness depending on δ), one has $\mathcal{P}_{\text{pdl}} = 1$. This implies that $\lim_{\varepsilon \rightarrow 0} G(\varepsilon) = 0$.

Finally, we examine the situation when $\delta = 0$ and $\varepsilon \rightarrow 0$. In the classification diagram in Figure 19, this corresponds to approaching the origin along the ε -axis. By the averaging principle alluded to earlier [86, Thm. 2.1], the process X converges in probability, uniformly on compact time intervals, to the deterministic solution of the averaged problem

$$\begin{aligned} \dot{x}(t) &= \frac{1}{2}(U_0 + U_1)x(t) = \begin{pmatrix} 0 & 1/2 \\ -1/2 & 0 \end{pmatrix} x(t), \\ x(0) &= x_0. \end{aligned}$$

The matrices U_0 and U_1 contribute equally to the averaged matrix $\frac{1}{2}(U_0 + U_1)$ because $\lambda_0 = \lambda_1$. The eigenvalues of the averaged matrix are $\pm \frac{i}{2}$, with zero real part. In this doubly singular situation, the previously observed dichotomy is broken: For every $x_0 \neq 0$, the trajectory of the solution to the averaged problem is a periodic orbit, more precisely a circle of radius $\|x_0\|$ centered at the origin.

As second example for a piecewise deterministic Markov process, we are going to use a logistic growth model with random switching. Just as our first example, this Markov process is characterized by random switching between two vector fields with a critical point in common. Unlike the first example, though, the vector fields share a compact trapping region of positive Lebesgue measure that gives rise to a nontrivial stationary distribution.

The logistic model is a classical model for the growth

of a population that is limited by the capacity of the environment to sustain the population. The model is described by the logistic differential equation $\dot{x}(t) = \mathcal{U}(x(t), r, p)$, where

$$\mathcal{U}(x, r, p) := rx(1 - x/p).$$

The time-dependent variable x represents the population size. The parameters r (the growth rate) and p (the carrying capacity) are assumed to be positive.

We consider the dynamical system induced by randomly switching between the logistic vector fields

$$\begin{aligned} u_0(x) &:= \mathcal{U}(x, \delta, 1), \\ u_1(x) &:= \mathcal{U}(x, 1, 2), \end{aligned} \quad (\mathcal{X}_{\text{pdp}})$$

at switching rates $\lambda_0 = \varepsilon$ and $\lambda_1 = 1$. Notice the asymmetry in the switching rates that will lead to the system spending more and more time in the regime governed by u_0 as ε approaches 0. In [114], random switching between the vector fields $\mathcal{U}(\cdot, p_-, p_-)$ and $\mathcal{U}(\cdot, p_+, p_+)$ was studied in detail, for parameters $p_- < 0$ and $p_+ > 0$ to the left and to the right of the transcritical bifurcation at $p = 0$. Even though the present setting is somewhat different, we will follow [114] quite closely.

For $r, p > 0$, the logistic vector field $\mathcal{U}(\cdot, r, p)$ has the equilibrium points 0 and p , which are unstable and asymptotically stable, respectively. Stability of 1 and 2 for u_0 and u_1 implies that the compact interval $[1, 2]$ is positively invariant under the switching dynamics, i.e. every switching trajectory starting in $[1, 2]$ stays in this interval for all positive times. Since, in addition, the Markov semigroup of (X, E) is Feller (see Proposition 2.1 in [20]), the Krylov–Bogoliubov method (Theorem 3.1.1 in [64]) yields the existence of a stationary distribution μ such that $\mu([1, 2] \times \{0, 1\}) = 1$. Moreover, by [9, Theorem 2] or by [20, Theorem 4.4], μ is the unique stationary distribution for (X, E) that assigns full measure to $(0, \infty) \times \{0, 1\}$. Finally, again by [9, Theorem 2], μ is absolutely continuous with respect to the product of Lebesgue measure on $(0, \infty)$ and counting measure on $\{0, 1\}$. Hence, μ admits a density ρ with respect to the latter measure.

For the invariant density $\rho_0(\cdot) := \rho(\cdot, 0)$, we consider the property

$$\mathcal{P}_{\text{bdd}} = \begin{cases} 1, & \text{if } \rho_0 \text{ is bounded on } (1, 2), \\ 0, & \text{if } \rho_0 \text{ is unbounded on } (1, 2). \end{cases}$$

By [11, Thm. 1], ρ_0 and $\rho_1 := \rho(\cdot, 1)$ are C^∞ smooth in the open interval $(1, 2)$ because u_0 and u_1 are smooth vector fields with no equilibrium points in $(1, 2)$. As a result, the corresponding probability fluxes $\varphi_i := \rho_i u_i$, $i \in \{0, 1\}$, satisfy the Fokker–Planck equations [85]

$$\varphi_i'(x) = - \left(\frac{\varepsilon}{u_0(x)} + \frac{1}{u_1(x)} \right) \varphi_i(x), \quad (19)$$

for all $x \in (1, 2)$. The ODE in (19) has the general solution

$$\varphi_i(x) = Cx^{-\frac{\varepsilon}{\delta}-1}(x-1)^{\frac{\varepsilon}{\delta}}(2-x), \quad x \in (1, 2),$$

hence

$$\begin{aligned} \rho_0(x) &= c_1 x^{-\frac{\varepsilon}{\delta}-2} (x-1)^{\frac{\varepsilon}{\delta}-1} (2-x), \\ \rho_1(x) &= c_2 x^{-\frac{\varepsilon}{\delta}-2} (x-1)^{\frac{\varepsilon}{\delta}}, \end{aligned}$$

for positive normalizing constant c_1 and c_2 . These formulae for ρ_0 and ρ_1 show that ρ_1 is always bounded on $(1, 2)$. Furthermore, the invariant density ρ_0 has a singularity at the equilibrium point 1 of u_0 if and only if $\varepsilon < \delta$. We obtain the following cases:

- (I) If $\delta \leq \varepsilon$, then $\mathcal{P}_{\text{bdd}} = 1$.
- (II) If $\delta > \varepsilon$, then $\mathcal{P}_{\text{bdd}} = 0$.

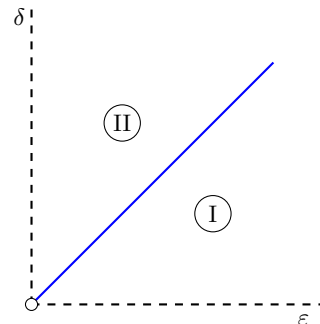


FIG. 20: Classification diagram with respect to the property \mathcal{P}_{bdd} . The two regions I and II correspond to the cases (I) (bounded) and (II) (unbounded). The blue ray separating the regions (I) and (II) belongs to region (I). The property is not well-defined on the axes.

This dichotomy admits the following heuristic explanation: If ε (the rate of switching away from the vector field u_0) is small compared to δ (the contraction rate of u_0 at its equilibrium point $x = 1$), then a large amount of probabilistic mass accumulates in the vicinity of the equilibrium point; a singularity at $x = 1$ is formed. Conversely, if ε is large in comparison with δ , the system switches sufficiently often away from u_0 to prevent a strong accumulation of probabilistic mass near $x = 1$; the invariant density ρ_0 stays bounded.

In the singular case $\varepsilon = 0$, no switching away from u_0 takes place. The process (X, E) still has a unique stationary distribution on $(0, \infty) \times \{0, 1\}$, namely the product of the Dirac measure at $x = 1$ and the measure $(1, 0)$ on $\{0, 1\}$. Of course, this distribution no longer has a probability density function with respect to the product of Lebesgue measure on $(0, \infty)$ and counting measure on $\{0, 1\}$. It follows that the property \mathcal{P}_{bdd} cannot be studied on the δ -axis.

If $\delta = 0$, the vector field u_0 is constantly equal to zero. As long as $\varepsilon > 0$, the system alternates between flowing along u_1 and staying put. The unique stationary distribution on $(0, \infty) \times \{0, 1\}$ is then the product of the Dirac measure at the equilibrium point $x = 2$ of the measure $(\frac{1}{1+\varepsilon}, \frac{\varepsilon}{1+\varepsilon})$ on $\{0, 1\}$. Again, \mathcal{P}_{bdd} cannot be meaningfully studied. Finally, in the doubly singular case $\varepsilon = \delta = 0$,

one obtains an infinite family of stationary distributions $(\mu^x)_{x>0}$, where μ^x is the product of the Dirac measure at x and the measure $(1, 0)$ on $\{0, 1\}$.

For switching systems in dimension greater than one, the set of singularities of invariant densities can have a much richer structure than the one exhibited here (see [10] for a simple yet nontrivial example in 2D). This can result in more complex classification diagrams with respect to a suitably defined version of \mathcal{P}_{bdd} .

We conclude this subsection with some remarks on the two examples presented above. We also hint at additional topics in the field of piecewise deterministic processes where double limits may be fruitfully studied.

In the first example, we saw that switching between vector fields of a certain kind (stable, in our example) can result in a dynamical system of a very different kind (unstable). In the same vein, for a Lotka–Volterra system of two competing species, it is shown in [24] that switching between two environments that both favor the same species can even lead to the extinction of this species. The articles [24], [165], and [164] together provide a clear picture of which parameter choice results in which long-term behavior for the Lotka–Volterra system. It is thus possible to represent the interplay of the parameters by a double-limit diagram.

The boundedness property for invariant densities is straightforward to study for piecewise deterministic processes of spatial dimension one [11]. In higher dimensions, a regularity theory for invariant densities is still missing. However, the double-limits framework developed in this article can also be meaningfully applied to other ergodic properties, e.g. the number of stationary distributions, absolute continuity of stationary distributions with respect to a suitable reference measure, or exponential ergodicity. When it comes to the number of stationary distributions, an essential tool is the theory of stochastic persistence [18], which gives criteria for the existence of a stationary distribution on the complement of an invariant closed subset of the phase space (the *extinction set*). In [23] and [200], this theory – originally devised for Markov processes in general – has been further developed in the context of piecewise deterministic processes.

In general, there is a lack of precise necessary conditions for absolute continuity and exponential ergodicity of the stationary distribution. Besides, neither of these properties is affected by the rates of switching, which makes it imperative to link both of the small parameters ε and δ to the vector fields in order to obtain a nontrivial double-limit diagram. Apart from [20] and [9], absolute continuity for piecewise deterministic processes was studied for instance in [63] and [161], where the process X is allowed to have jumps. Sufficient conditions for exponential ergodicity in total-variation distance were given in [20], [153], and [21]; and for exponential ergodicity in Wasserstein distance in [22] and [58].

Other types of switching processes have been studied in the literature, some of them abundantly: switch-

ing between PDEs [150], non-Markovian switching [154], switching between diffusions [217], etc. All of these classes of stochastic processes are amenable to the double-limit approach proposed in this article.

We have already seen in the current context, that one expects double limit problems for stochastic systems to be directly linked to double limits for Fokker–Planck (or Kolmogorov) equations. We shall now continue with this theme and focus in the next two subsections on problems arising from various classes of partial differential equations (PDEs).

3.5. Matched Asymptotic Expansions & BVPs

Two-parameter singularly perturbed systems of differential equations have been widely studied from the analytical as well as from the numerical viewpoint (see [57, 95, 103, 130, 179, 183, 184, 192, 206, 210] and references therein). In most cases, the singularity is attributed to the presence of small parameters in front of the derivative terms; however, as shown in [190], this is not a necessary condition. This also applies to the problem presented in this section.

We start with a PDE problem, which still naturally links to ODEs and classical double limit fast-slow systems. We consider the following boundary value problem:

$$\begin{aligned} u_{XX} &= \frac{\lambda}{(1+u)^2} \left[1 - \frac{\varepsilon^2}{(1+u)^2} \right], & X \in [-1, 1], & (\mathcal{X}_{\text{mes}}) \\ u &= 0, & X = \mp 1. \end{aligned}$$

Equation $(\mathcal{X}_{\text{mes}})$ describes the steady states associated to a second-order parabolic PDE problem arising in the context of Micro-Electro Mechanical Systems (MEMS) [160]. In particular, the function $u(X)$ represents the deflection of an elastic membrane towards a ground plate under the action of an electric potential described by the parameter $\lambda > 0$, while $0 < \varepsilon \ll 1$ appears as a regularization parameter.

The bifurcation diagram associated to $(\mathcal{X}_{\text{mes}})$ consists of two branches of stable equilibria separated by a third, intermediate branch of unstable equilibria (see Figure 21a). The middle and upper branch meet at a saddle-node bifurcation point $\lambda_*(\varepsilon)$. A steady-state solution exists for every $\lambda > 0$, and the presence of the regularizing ε -dependent term in $(\mathcal{X}_{\text{mes}})$ guarantees that for any ε the solution is bounded below by $u = -1 + \varepsilon$; see Figure 21b.

In [160], the authors have studied $(\mathcal{X}_{\text{mes}})$ both analytically, using matched asymptotic expansions to construct solutions, and numerically, investigating the structure of the ε -dependent bifurcation diagram. However, the analytical motivation behind logarithmic switchback terms in the expansions, as well as a detailed resolution of the bifurcation diagram for very small values of ε , were left as challenging open questions. In [119], a detailed asymptotic resolution of 21a, both in the singular limit of $\varepsilon = 0$

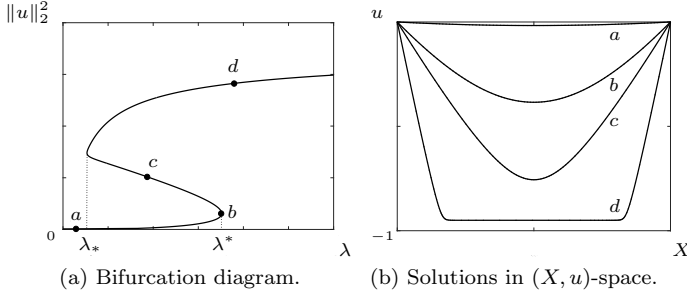


FIG. 21: (a) Numerically computed bifurcation diagram of the one-dimensional membrane model, $(\mathcal{X}_{\text{mes}})$, for $\varepsilon = 0.05$. (b) Corresponding solutions in (X, u) -space.

and for ε positive and sufficiently small, is accomplished through separate investigation of three distinct, yet overlapping, regions in the diagram, allowing us to tackle these questions.

To that end, we first reformulate the boundary value problem $(\mathcal{X}_{\text{mes}})$ in a dynamical systems framework; then, identification of two main parameters in the resulting equations yields a two-parameter singular perturbation problem. Careful asymptotic analysis of that problem allows us to identify the corresponding limiting solutions, and to show how the third branch in the diagram found for non-zero ε emerges from the singular limit of $\varepsilon = 0$, where only the lower and the middle branch are present. On that basis, we prove the existence and uniqueness of solutions close to these limiting solutions.

We reformulate $(\mathcal{X}_{\text{mes}})$ as a first-order system by re-labeling u with x , introducing the variable $y = x_X$, and appending the trivial dynamics for the spatial variable X , which we relabel as ξ , and ε . Moreover, we desingularize the flow near $x = -1$ and define a shift in x via $\tilde{x} = 1 + x$, which translates the singularity to $\tilde{x} = 0$. Omitting the tilde and denoting differentiation with respect to the new independent variable by a prime, we obtain

$$x' = x^4 y, \quad (20a)$$

$$y' = \lambda(x^2 - \varepsilon^2), \quad (20b)$$

$$\xi' = x^4, \quad (20c)$$

$$\varepsilon' = 0, \quad (20d)$$

subject to the boundary conditions $x = 1$ at $\xi = \mp 1$. For $\varepsilon = 0$, this systems admits the line of degenerate equilibria

$$\mathcal{S}^0 = \{(0, y, \xi, 0) \mid y \in \mathbb{R}, \xi \in \mathbb{R}\}. \quad (21)$$

When $\lambda = 0$, there is an additional manifold of equilibria for (20a)-(20b) given by

$$\mathcal{M}^0 := \{(x, 0, \xi, 0) \mid x \in \mathbb{R}^+, \xi \in \mathbb{R}\}. \quad (22)$$

As it turns out, in two of the three regions we investigate

it is useful to introduce a rescaled variable $\tilde{y} = \delta y$, where

$$\delta = \sqrt{\frac{\varepsilon}{\lambda}}. \quad (23)$$

Omitting the tilde for sake of simplicity, System (20) hence becomes

$$x' = x^4 y, \quad (24a)$$

$$y' = \varepsilon(x^2 - \varepsilon^2), \quad (24b)$$

$$\xi' = \delta x^4, \quad (24c)$$

$$\varepsilon' = 0. \quad (24d)$$

We observe that (24) is a fast-slow system, where x is fast and y is slow. The nature of ξ , however, depends on δ : in particular, ξ is fast when $\delta = \mathcal{O}(1)$, and it is slow when $\delta = \mathcal{O}(\varepsilon)$. For $\delta = 0$, the manifolds \mathcal{S}^0 and \mathcal{M}^0 represent two branches of the critical manifold for (24). Since \mathcal{S}^0 is not normally hyperbolic, and the reduced flow on it is highly degenerate, one can apply the blow-up method to describe the dynamics of (24) in its vicinity [77, 78, 141]. Such method has proved to be particularly useful when tackling two-parameter perturbed systems [137, 170]. To this aim, we introduce the following blow-up transformation:

$$x = \bar{r}\bar{x}, \quad y = \bar{y}, \quad \xi = \bar{\xi}, \quad \text{and} \quad \varepsilon = \bar{r}\bar{\varepsilon}, \quad (25)$$

where $(\bar{y}, \bar{\xi}) \in \mathbb{R}^2$ and $(\bar{x}, \bar{\varepsilon}) \in S^1$, i.e., $\bar{x}^2 + \bar{\varepsilon}^2 = 1$. The vector field induced by (25) on the cylindrical manifold in $(\bar{x}, \bar{y}, \bar{\xi}, \bar{\varepsilon}, \bar{r})$ -space is best described in coordinate charts; in particular, to carry out our analysis we require the two following charts:

$$K_1 : (x, y, \xi, \varepsilon) = (r_1, y_1, \xi_1, r_1 \varepsilon_1), \quad (26a)$$

$$K_2 : (x, y, \xi, \varepsilon) = (r_2 x_2, y_2, \xi_2, r_2). \quad (26b)$$

We note that the phase-directional chart K_1 describes the “outer” regime, which corresponds to the transient from $x = 1$ to $x = 0$ approaching \mathcal{S}^0 , while the rescaling chart K_2 covers the “inner” regime where $x \approx 0$, in the context of (24). The corresponding dynamics are given by

$$K_1 : \begin{cases} r_1' = r_1 y_1, \\ y_1' = \varepsilon_1(1 - \varepsilon_1^2), \\ \xi_1' = \delta r_1, \\ \varepsilon_1' = -\varepsilon_1 y_1. \end{cases} \quad K_2 : \begin{cases} x_2' = x_2^4 y_2, \\ y_2' = x_2^2 - 1, \\ \xi_2' = \delta r_2 x_2^4, \\ r_2' = 0. \end{cases} \quad (27)$$

In order to construct singular solutions, we define the entry and exit sections in K_1

$$\Sigma_1^{\text{in}} := \{(\rho, y_1, \xi_1, \varepsilon_1) \mid y_1 \in [y_-, y_+], \xi_1 \in [\xi_-, \xi_+], \varepsilon_1 \in [0, \sigma]\}, \quad (28)$$

$$\Sigma_1^{\text{out}} := \{(r_1, y_1, \xi_1, \sigma) \mid r_1 \in [0, \rho], y_1 \in [y_-, y_+], \xi_1 \in [\xi_-, \xi_+]\}, \quad (29)$$

where $0 < \rho < 1$ and $0 < \sigma < 1$ are appropriately defined constants, while y_{\mp} and ξ_{\mp} are real constants, with $y_- < -\frac{2}{\sqrt{3}}$ and $y_+ > \frac{2}{\sqrt{3}}$. Translating Σ_1^{out} in terms of K_2 -coordinates, we obtain the section

$$\Sigma_2^{\text{in}} := \{(\sigma^{-1}, y_2, \xi_2, r_2) \mid y_2 \in [y_-, y_+], \xi_2 \in [\xi_-, \xi_+], r_2 \in [0, \rho\sigma]\}. \quad (30)$$

In terms of matched asymptotics, such sections describe the transition between outer and inner regions. In particular, the outer regime corresponds to the area limited by Σ_1^{in} and Σ_1^{out} in K_1 , while the inner regime is limited by Σ_2^{in} and the hyperplane $\{y = 0\}$ in K_2 .

Solutions to $(\mathcal{X}_{\text{mes}})$ arise as perturbations of singular solutions obtained in the limit of $\varepsilon = 0$. Such solutions are constructed by analyzing the dynamics in charts K_1 and K_2 separately in the limit as $\varepsilon \rightarrow 0$. In particular, solutions are constructed via two strategies:

Strategy 1. We consider two sets of boundary conditions, corresponding to suitable intervals of y -values that are defined at $\xi = -1$ and $\xi = 1$, respectively. Flowing these two sets of boundary conditions forward and backward, respectively, we verify the transversality of the intersection of the two resulting manifolds at $\xi = 0$. Each initial y -value y_0 for which these two manifolds intersect gives a solution to the boundary value problem $(\mathcal{X}_{\text{mes}})$.

Strategy 2. Since all such solutions are even, we can focus our attention on the ξ -interval $[-1, 0]$, with boundary conditions $x(-1) = 1$ and $y(0) = 0$. The set of initial conditions at $\xi = -1$ and $x = 1$, but with arbitrary initial y -value y_0 , is then tracked forward up to the hyperplane $\{y = 0\}$. The resulting manifold is naturally parametrized by $x(y, \varepsilon, \delta, y_0)$ and $\xi(y, \varepsilon, \delta, y_0)$; the unique ‘‘correct’’ value $y_0(\varepsilon, \delta)$ corresponding to a solution to $(\mathcal{X}_{\text{mes}})$ is then obtained by solving $\xi(y_0, \varepsilon, \delta) = 0$ under the constraint that $y(y_0, \varepsilon, \delta) = 0$.

We distinguish three types of singular solutions to $(\mathcal{X}_{\text{mes}})$ (see Figure 22):

Type M1. Solutions of type M1 (indicated in blue in the following figures) satisfy $x = 0$ for $X \in I$, where I is an interval centered at $X = 0$. They occur in two subtypes: the ones corresponding to $\lambda = \mathcal{O}(\varepsilon)$ have constant finite slope w outside of I , while the ones corresponding to $\lambda = \mathcal{O}(1)$ vanish on $I = (-1, 1)$.

Type M2. Solutions of type M2 (indicated in green) are those of slope $y \equiv \mp 1$. These solutions reach $\{x = 0\}$ at one point only, namely at $X = 0$.

Type M3. Solutions of type M3 (indicated in black) never reach $\{x = 0\}$.

For $\varepsilon > 0$, we divide the bifurcation diagram in $(\lambda, \|x\|_2^2)$, in terms of the original variable, into three

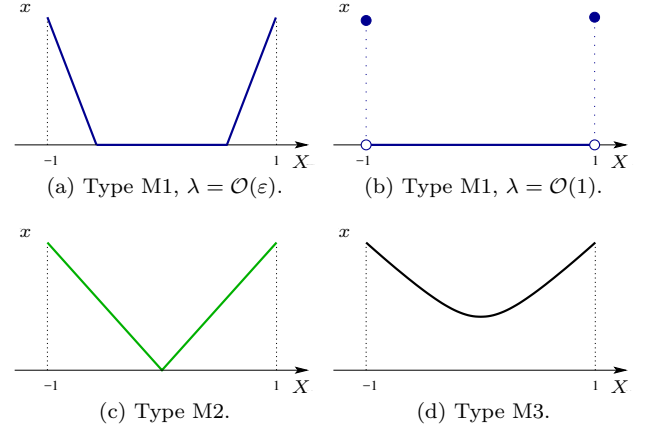


FIG. 22: Singular solutions to $(\mathcal{X}_{\text{mes}})$.

overlapping regions, as shown in Figure 23:

$$\mathcal{R}_1 := [0, 1] \times \left[\frac{2}{3} + \nu_1, 2 \right], \quad (31a)$$

$$\mathcal{R}_2 := [0, \varepsilon\lambda_2] \times \left[\frac{2}{3} - \nu_2, \frac{2}{3} + \nu_2 \right], \quad (31b)$$

$$\mathcal{R}_3 := [0, 1] \times \left[0, \frac{2}{3} + \nu_2 \right] \setminus [0, \varepsilon\lambda_3] \times \left[\frac{2}{3} - \nu_3, \frac{2}{3} + \nu_2 \right], \quad (31c)$$

with $\nu_2 > \nu_1 > 0$, $\nu_2 > \nu_3 > 0$, and $\lambda_2 > \lambda_3 > 0$ large.

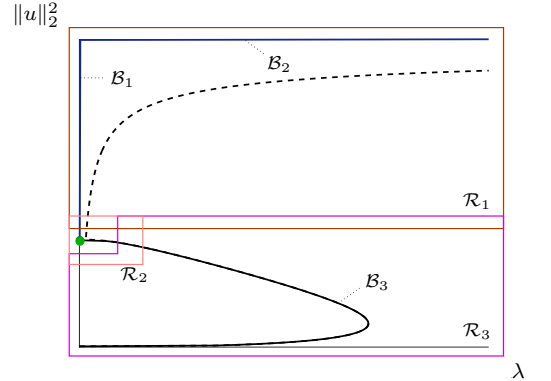


FIG. 23: Covering of the bifurcation diagram for $(\mathcal{X}_{\text{mes}})$ by regions \mathcal{R}_1 (brown), \mathcal{R}_2 (pink), and \mathcal{R}_3 (magenta). The branches of solutions to $(\mathcal{X}_{\text{mes}})$ for $\varepsilon = 0.01$ (dotted curve) and $\varepsilon = 0$ (solid curve) are displayed. For $\varepsilon = 0$, the upper branch reduces to the union of a vertical part \mathcal{B}_1 , corresponding to $\lambda = \mathcal{O}(\varepsilon)$, and a horizontal part \mathcal{B}_2 which corresponds to $\lambda = \mathcal{O}(1)$. The green dot at B represents the singular solution of type M2 for $\lambda = 0$. The black curve for type M3-solutions is labeled \mathcal{B}_3 .

In our analysis, we consider $\lambda \in [0, 1]$. In region \mathcal{R}_3 , away from the point $B = (0, \frac{2}{3})$, the perturbation with ε is regular, and we consider λ and δ as the two main parameters for our investigation. In regions \mathcal{R}_1 and \mathcal{R}_2 , singular solutions exist only for $\lambda \geq \frac{3}{4}\varepsilon$ or, equivalently,

for $\delta \leq \frac{2}{\sqrt{3}}$. Hence, in these regions, we need to take $\lambda \in [\frac{3}{4}\varepsilon, 1]$, i.e. $\delta \in [\sqrt{\varepsilon}, \frac{2}{\sqrt{3}}]$; see Figure 24. The two main parameters we consider in our proofs are here ε and δ . We define

$$\mathcal{P}_{ss} := \text{singular solutions of (24) exist.} \quad (32)$$

In Regime (I), such property is satisfied and singular solutions of type M1 and M2 exist, whereas in Regime (IV) there are no singular solutions. Two special cases are represented by Regime (II) (corresponding to \mathcal{B}_1), where singular solutions of type I exist, and Regime (III) (corresponding to $\mathcal{B}_2 \cup \mathcal{B}_3$), where we recover singular solutions of type M1 and M3.

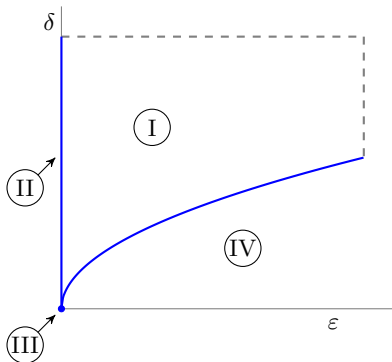


FIG. 24: Classification diagram of $(\mathcal{X}_{\text{mes}})$ with respect to the property \mathcal{P}_{ss} in $\varepsilon\delta$ -space. Regime (I) is bounded below by $\{\delta = \sqrt{\varepsilon}\}$ (blue curve) and above by $\{\delta = \frac{2}{\sqrt{3}}\}$ (dashed gray line). Regime (I): two singular solutions of type M1 and M2 exist. Regime (II): singular solutions of type M1 exist. Regime (III): singular solutions of type M2 and M3 exist. Regime (IV): no singular solutions exist.

By definition, $\delta = 0$ occurs only when $\varepsilon = 0$. The corresponding, highly degenerate limit gives a singular orbit of type M1 with very singular structure, as shown in 22b. Hence, the whole line \mathcal{B}_2 corresponds to that one singular solution.

In \mathcal{R}_1 , we construct singular solutions and show their persistence for $\varepsilon > 0$ small, using Strategy 1 as follows. For a fixed $\lambda \in [\frac{\varepsilon}{\delta_1^2}, 1]$ with $0 < \delta_1 < \frac{2}{\sqrt{3}}$, i.e. $\delta < \frac{2}{\sqrt{3}}$, the presence of a saddle-node equilibrium for the (x_2, y_2) -subsystem in chart K_2 at $(1, 0)$, on which the reduced flow w.r.t. ξ_2 occurs, allows us to determine the unique, correct boundary value for y at $\xi = -1$ by following the stable manifold of such equilibrium, which does not depend on ε and does therefore not change for $\varepsilon > 0$, backwards until $\Sigma_2^{\text{in}} = \Sigma_1^{\text{out}}$, and then tracking the flow in chart K_1 backwards until $\xi_1 = -1$. The intrinsic symmetry of the problem allows us to apply the same argument to the right part of the orbit, tracking the unstable manifold of the equilibrium $(x_2, y_2) = (1, 0)$ and following the flow in chart K_1 until $\xi_1 = 1$. When $0 \leq \delta < \hat{\delta}$, the proof is analogous except for the fact that we must

rescale $\delta = \sqrt{\varepsilon}\tilde{\delta}$ and obtain a slower reduced flow. The assumption that $\delta < \frac{2}{\sqrt{3}}$ ensures a non-trivial slow drift (i.e. the portion of the orbit where $x = 0$ does not reduce to a point), which allows us to apply the Exchange Lemma to infer persistence of solutions for $0 < \varepsilon \ll 1$.

For $\frac{1}{\sqrt{\lambda_2}} \leq \delta \leq \delta_1$, i.e. in \mathcal{R}_2 , we show the existence of two unique type M1 and type M2 solutions which coincide when $\delta = \frac{2}{\sqrt{3}}$. The proof consists of two parts: we first consider a small neighborhood of $\delta_* = \frac{2}{\sqrt{3}}$, i.e. of $\lambda = \frac{3}{4}\varepsilon$, where the saddle-node bifurcation occurs. We define a suitable bifurcation equation, which describes the transition from solutions which limit on type M1-solutions to those which limit on solutions of type M2. Such equation is constructed by imposing that $\xi_2(y_0, \varepsilon, \delta) = 0$ when $y(y_0, \varepsilon, \delta) = 0$, i.e. using Strategy 2. Based on that equation, we infer the presence of the saddle-node bifurcation, and we calculate the expansion of the corresponding λ -value λ_* . This expansion presents logarithmic switchback terms due to both a resonance phenomenon in chart K_1 and the passage close to the saddle point $(x_2, y_2) = (1, 0)$. In a second step, we consider the branch of solutions that limit on type M2-solutions for the remaining values of λ in \mathcal{R}_2 . That branch is then shown to connect to solutions that are covered by region \mathcal{R}_3 , for which $\delta = 0$. In that case, the type M2-solution constructed in \mathcal{R}_2 collapses onto the line $\{y_1 = 0\}$, which leads to singular dynamics in K_1 . Since such singular nature is due to the w -rescaling introduced to obtain System (24), this regime is better studied using System (20) and replacing $\varepsilon = \delta^2\lambda$. Since this region contains a neighborhood of $(\delta, \lambda) = (0, 0)$, we must perform an additional blow-up of $(u, \lambda) = (0, 0)$ and split \mathcal{R}_3 into two sub-regions: for $\lambda \in [\tilde{\lambda}, \lambda^*]$ with $\tilde{\lambda} > 0$ and $\delta = 0$, we can show the existence of a unique singular solution of type M3 which perturbs regularly when $0 < \delta \ll 1$ (in particular $\delta \leq \frac{1}{\sqrt{\lambda_3}}$ in \mathcal{R}_3). When $\lambda \in [0, \tilde{\lambda}]$, i.e. when \mathcal{R}_3 and \mathcal{R}_2 overlap, we have a singular solution of type M2 as $\lambda \rightarrow 0$, and of type M3 as $\delta \rightarrow 0$.

In summary, even unfolding a rather innocent-looking PDE problem via spatial dynamics in one dimension leads to a highly interesting double limit problem. In the next section, we continue this theme and consider a multi-component stationary PDE problem.

3.6. Fast Reaction Limits

A variety of biological and ecological phenomena present different intrinsic time-scales, and typically some processes are faster than others. The singular limit, or fast reaction limit, expresses the fact that instantaneous dynamics is also included in the system. For instance, in a population, there can be a dichotomy of two groups, and switching between them may be possible. Compared to other interactions, the switch may seem *instantaneous*

and give rise to interesting effects such as an aggregation of individuals or a population density pressure [54, 105]. Fast reaction limits have also been studied in other contexts, such as reversible and irreversible chemical reactions [49, 50], bacteria proliferation [104], proteins localisation in stem cell division [102], but also to model the Neolithic spread of farmers in Europe [79, 80].

In the context of predator–prey interactions, the expression of widely used functional responses can also come out of a systematic process in which one starts with a system of more than two equations with simple reaction terms and performs one [28, 113, 151, 168] or more limits [70, 93].

We consider here the cross-diffusion system, known as Shigesada–Kawasaki–Teramoto (SKT) model [196], proposed to account for stable inhomogeneous steady states exhibiting spatial segregation between two species competing for resources. We refer to [53, 146] and references therein for more details. The system is given by

$$\begin{aligned}\partial_t u - \Delta_x ((d_1 + d_{12}v)u) &= f(u, v)u, \\ \partial_t v - \Delta_x ((d_2 + d_{21}u)v) &= g(u, v)v,\end{aligned}\quad (33)$$

endowed with initial conditions and homogeneous Neumann boundary conditions. The quantities $u(t, x), v(t, x) \geq 0$ represent the population densities of two species at time t and position x , confined on a bounded and connected domain $\Omega \subset \mathbb{R}^N$. The movements of the individuals on the domain are described by non-linear cross-diffusion terms: the positive coefficients d_1, d_2 refer to the (standard) diffusion, while the non-negative cross-diffusion coefficients d_{12}, d_{21} stand for competition pressure. The reaction terms describe the growth and the interaction of the two species, where

$$\begin{aligned}f(u, v) &= r_1 - a_1 u - b_1 v, \\ g(u, v) &= r_2 - b_2 u - a_2 v,\end{aligned}\quad (34)$$

with the non-negative coefficients r_i, a_i, b_i ($i = 1, 2$) being the intrinsic growth, the intra-specific competition and the inter-specific competition rates.

Model (33) falls into the class of quasilinear parabolic systems for which even the existence problem of solutions is not trivial. When $d_{21} = 0$ (triangular cross-diffusion system), it has been shown [116, 121] that the solutions of (33) can be approximated in a finite time interval by those of a three-component reaction–diffusion system if the solutions are bounded and provided that a suitable parameter is small enough. The rigorous proof of the convergence of solutions of the three-component reaction–diffusion system towards the solutions of a triangular cross-diffusion systems of two equations has been initially given in dimension $N = 1$ [59], and later generalized to a wider set of admissible reaction terms and in any dimension [71].

The convergence of the stationary steady states of the fast-reaction systems towards the ones of the cross-diffusion system has been also investigated by looking

at bifurcation diagrams with respect to different bifurcation parameters [121, 146]. In particular, it has been observed that the bifurcation structure of the fast-reaction expands and converges as the time scale parameter becomes smaller, sometimes going through major qualitative changes.

When $d_{21} > 0$, the full cross-diffusion system (33) can be obtained, at least formally, as the singular-limit of a four-component fast-reaction system involving two small time scale parameters ε, δ . In this case both species are split into quiet and active states, denoted by u_1, v_1 and u_2, v_2 respectively. Hence, we have that $u := u_1 + u_2, v := v_1 + v_2$. The resulting reaction–diffusion system is

$$\begin{aligned}\partial_t u_1 - d_1 \Delta_x u_1 &= f(u, v)u_1 + \frac{1}{\varepsilon} h(u_1, u_2, v), \\ \partial_t u_1 - \hat{d}_1 \Delta_x u_2 &= f(u, v)u_2 - \frac{1}{\varepsilon} h(u_1, u_2, v), \\ \partial_t v_1 - d_2 \Delta_x v_1 &= g(u, v)v_1 + \frac{1}{\delta} k(u, v_1, v_2), \\ \partial_t v_2 - \hat{d}_2 \Delta_x v_2 &= g(u, v)v_2 - \frac{1}{\delta} k(u, v_1, v_2),\end{aligned}\quad (\mathcal{X}_{\text{fr}})$$

together with initial conditions and homogeneous Neumann boundary conditions. Active states are supposed to have a larger diffusion coefficient than the corresponding quiet state. In particular, we assume that the diffusion coefficients of the active states are given by $\hat{d}_1 := d_1 + d_{12}M_2$ and $\hat{d}_2 := d_2 + d_{21}M_2$, where M_1, M_2 are positive constants such that $0 \leq u(t, x) \leq M_1, M_1 \geq r_1/a_1$ and $0 \leq v(t, x) \leq M_2, M_2 \geq r_2/a_2$ in $\mathbb{R} \times \Omega$. The functions h, k describing the switch between the states are

$$\begin{aligned}h(u_1, u_2, v) &= \left(1 - \frac{v}{M_2}\right) u_2 - u_1 \frac{v}{M_2}, \\ k(u, v_1, v_2) &= \left(1 - \frac{u}{M_1}\right) v_2 - v_1 \frac{u}{M_1},\end{aligned}\quad (35)$$

while the time scale parameters ε, δ describe that the switch between the two different states happens much faster than the other processes.

At a formal level, when $\varepsilon \rightarrow 0$, system $(\mathcal{X}_{\text{fr}})$ reduces to an intermediate three-component reaction–cross-diffusion system in the variables u, v_1, v_2 . The equation for u represents cross-diffusion, while the other time scale parameter δ is still present in the equations for v_1, v_2 . Letting $\delta \rightarrow 0$, the intermediate three-component system reduces to the full cross-diffusion system. The same considerations hold if we let $\delta \rightarrow 0$ first, and $\varepsilon \rightarrow 0$. In the time scale parameter plane (Figure 25), the first quadrant corresponds to the four-equation system $(\mathcal{X}_{\text{fr}})$. The ε -axis corresponds to the reduced system with three equations for u_1, u_2, v , being the last equation with cross-diffusion. The δ -axis corresponds to the reduced system with three equations for u, v_1, v_2 , being the first equation with cross-diffusion. Finally, the origin corresponds to system (33) with two cross-diffusion equations.

To the best of the authors' knowledge, there are currently no rigorous results of convergence of solutions of

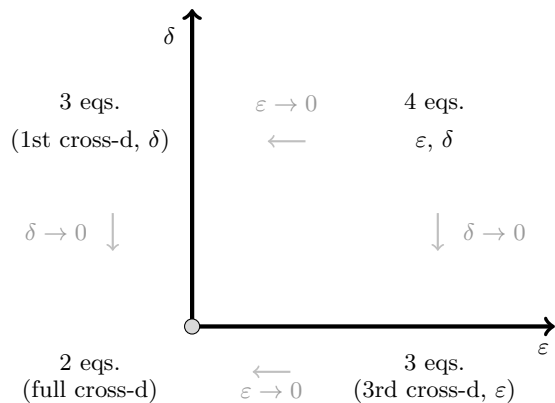


FIG. 25: Schematic representation of the systems of PDEs in the $\varepsilon\delta$ -plane. The first quadrant corresponds to the four-equation system (\mathcal{X}_{fr}). The ε -axis corresponds to the reduced system with three equations for u_1, u_2, v , being the last equation with cross-diffusion. The δ -axis corresponds to the reduced system with 3 equations for u, v_1, v_2 , being the first equation with cross-diffusion. Finally, the origin corresponds to system (33) with two cross-diffusion equations.

the four-component reaction–diffusion systems to the solutions of the full cross-diffusion system. From a numerical point of view, despite a greater number of equations, the structure of system (\mathcal{X}_{fr}) is simpler than the cross-diffusion system (33), since it presents standard diffusion terms. For suitable small values of the time scale parameters ε, δ that leads to a “good” approximation of the cross-diffusion system (33), the four-component fast-reaction system tends to be more tractable. In order to establish how accurate is the approximation, we look at the bifurcation structure of stationary solutions when ε, δ become small.

On the one hand, system (33) admits the homogeneous coexistence state (u_*, v_*) where

$$u_* = \frac{r_1 a_2 - r_2 b_1}{a_1 a_2 - b_1 b_2}, \quad v_* = \frac{r_2 a_1 - r_1 b_2}{a_1 a_2 - b_1 b_2},$$

which is positive for suitable parameter values (see [53, 146]). It is known that the homogeneous solution undergoes some bifurcations under parameter variation, and branches of non-homogeneous solutions originate at these bifurcation points which correspond to different spatial distributions (patterns) of the species on the domain.

On the other hand, also system (\mathcal{X}_{fr}) admits the homogeneous coexistence state $(u_{1*}, u_{2*}, v_{1*}, v_{2*})$, given by

$$\begin{aligned} u_{1*} &= u_* \left(1 - \frac{v_*}{M_2} \right), & u_{2*} &= u_* \frac{v_*}{M_2}, \\ v_{1*} &= v_* \left(1 - \frac{u_*}{M_1} \right), & v_{2*} &= v_* \frac{u_*}{M_1}. \end{aligned}$$

The homogeneous coexistence state turns out to be independent of the parameters ε, δ . However, the number

r_2	a_1	a_2	b_1	b_2	d	d_{12}	d_{21}	M_1	M_2
5	2	3	5	4	0.03	3	3	5	2

TABLE I: Set of parameter values relevant to 27. The set $r_i, a_i, b_i, (i = 1, 2)$ corresponds to the strong-competition case ($a_1 a_2 - b_1 b_2 < 0$), namely the homogeneous coexistence state is unstable for the reaction part.

and the position of the bifurcation points on the homogeneous branch, and hence the global bifurcation structure, changes depending on the time scale parameters. Then, we say that the cross-diffusion system (33) and the four-component fast-reaction system (\mathcal{X}_{fr}) are equivalent if they have the same property

$$\mathcal{P}_{fr} := \begin{array}{l} \text{number of bifurcation points} \\ \text{on the homogeneous branch w.r.t.} \\ \text{the bifurcation parameter.} \end{array}$$

In the following, we select a set of parameters already used in [53] and reported in Table I. It corresponds to the strong competition case $a_1 a_2 - b_1 b_2 < 0$, in which the homogeneous coexistence state is unstable in absence of diffusion. However, stable non-homogeneous solutions arise on branches originating from bifurcation points on the homogeneous branch. In Figures 26a–26e we show different bifurcation diagrams obtained for smaller values of the parameters ε, δ , considering r_1 as bifurcation parameter and fixing the other parameter values, while Figure 26f corresponds to the non-triangular cross-diffusion system (33).

As shown in Figure 26, considering the parameter set in Table I, we have that $\mathcal{P}_{fr} = 2, 4$. In Figure 27 the qualitative classification diagram of system (\mathcal{X}_{fr}) with respect to the property \mathcal{P}_{fr} in the $\varepsilon\delta$ -plane is shown. The $\varepsilon\delta$ -plane can be split into two regions. Note also that in general the $\varepsilon\delta$ -diagram is not symmetric with respect to the diagonal $\varepsilon = \delta$, but the intersections of the separation curves with the axis depend on the parameter set, in particular on the cross-diffusion coefficients. With different parameter sets, mainly with smaller standard diffusion coefficients d , one can obtain more bifurcation points on the homogeneous branch, and more zones in the $\varepsilon\delta$ -plane, but its structure remains qualitatively similar to Figure 27.

The same study can be performed for other fast-reaction systems with multiple time scales and their cross-diffusion limits [60, 70].

3.7. Coupled Oscillators

As the last example, we proceed to systems on networks. As discussed above, the presence of multiple time scales can lead to oscillations that are relevant in a variety of physical contexts; whether it is simple relaxation oscillations [94], mixed mode oscillations [68], or other examples of oscillatory deterministic dynamics discussed

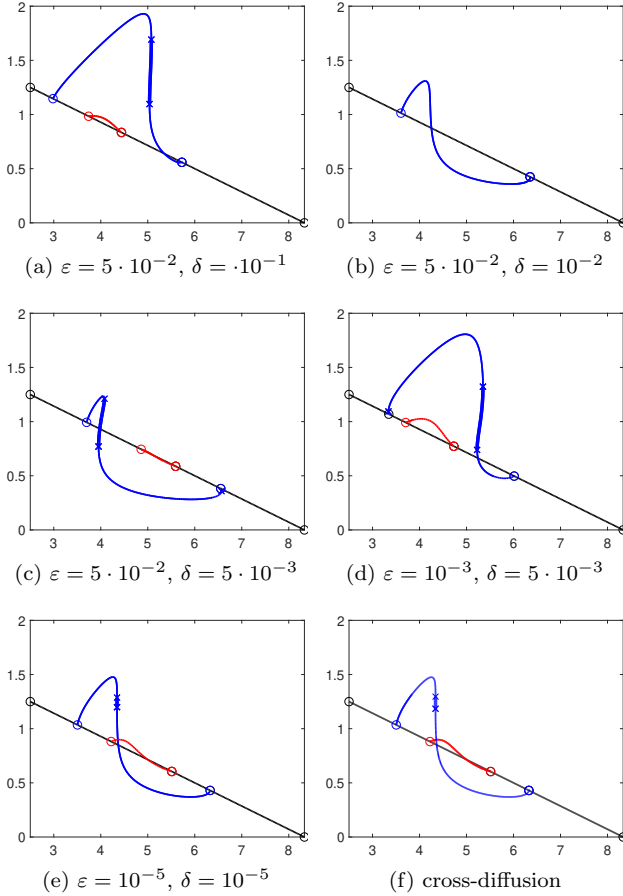


FIG. 26: Bifurcation diagrams with respect to the bifurcation parameter r_1 and the parameter set in Table I corresponding to different values of ε and δ . The black line corresponds to the homogeneous branch, while blue and red lines denote the bifurcating branches of non-homogeneous solutions. Bifurcation points are marked by circles.

in Sections 3.1 and 3.3. However, it is not only the oscillations themselves but also the *interaction* between different oscillatory processes that play an important role in many physical systems: These range from Huygens' synchronizing clocks [115] to coupled oscillatory dynamics in neuroscience [7, 109]. From a mathematical perspective, such systems can be understood as networks of coupled oscillators. In isolation, each node oscillator has state $z \in \mathbb{R}^d$ whose evolution is determined by a smooth ODE

$$z' := \frac{d}{dt} z = F(z) \quad (36)$$

that gives rise to an asymptotically stable limit cycle $\gamma \subset \mathbb{R}^d$. In a network, nodes interact non-trivially if there is an edge between the two nodes. Despite the dynamics of each node being fairly simple, the network dynamics, namely the dynamics of joint state of all nodes in the network, can be rich. While synchronization is

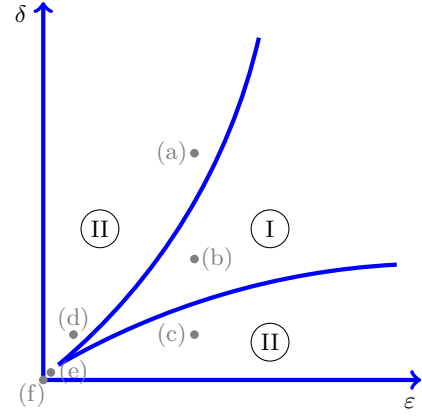


FIG. 27: Qualitative classification diagram of system (\mathcal{X}_{fr}) with respect to the property \mathcal{P}_{fr} in the $\varepsilon\delta$ -plane. Region I: two bifurcation points. Region II: four bifurcation points. Grey points correspond to the bifurcation diagrams in Figure 26.

probably one of the best understood dynamical phenomena in networks of coupled oscillators [40, 188, 201], even networks consisting of just a few fully symmetric nodes can give rise to complicated dynamics [39]. The network dynamics depend on both the intrinsic dynamical properties of each node and the network interactions. Here we will consider networks of weakly coupled relaxation oscillators, which have two small parameters: The time scale separation δ as an intrinsic property of the oscillators themselves and the coupling constant ε that is small by the assumption of weak coupling.

A network of N identical all-to-all coupled oscillators consists of N copies of (36) whose states $z_k \in \mathbb{R}^d$, $k \in \{1, \dots, N\}$, evolve according to

$$z'_k = F(z_k) + \frac{\eta}{N} \sum_{j=1}^N H(z_j, z_k), \quad (37)$$

where H is a smooth interaction function and η the coupling strength. If the coupling is weak, then the dynamics of this system on \mathbb{R}^{Nd} can be reduced to a lower-dimensional system [5]: If $\eta = 0$ then (37) has a normally hyperbolic invariant torus γ^N which persists for small coupling [109]. Specifically, there exists an $\eta_0 > 0$ such that for any $\eta < \eta_0$ the system (37) has an attracting normally hyperbolic invariant torus \mathbb{T} as a perturbation of $\gamma^N \subset \mathbb{R}^{Nd}$. In the following assume that η_0 is maximal with this property; note that, depending on H , this may allow for $\varepsilon_0 = \infty$, for example, for trivial coupling $H = 0$. The dynamics of (37) reduce to the interaction of N circular phase variables that evolve on \mathbb{T} , a phase oscillator network. The dynamics on the invariant torus are typically referred to as a phase reduction of (37); cf. [176, 187] for more details on how to compute these.

While a phase reduction is possible for any smooth oscillator, in many contexts the oscillators have particular

properties. Relaxation oscillators are characterized by two time scales leading to a combination of slow quasi-static and fast transitions. The most famous examples include the van der Pol oscillator [207] and FitzHugh–Nagumo oscillator [89, 175]. Consider a planar system (36) with state $z = (x, y)$ that evolves according to

$$\varepsilon x' = f(x, y) \quad (38a)$$

$$y' = g(x, y) \quad (38b)$$

where $f, g : \mathbb{R}^2 \rightarrow \mathbb{R}$ are smooth and $\varepsilon > 0$ is the time scale separation of the fast variable x and the slow variable y . Now assume that (38) gives rise to a family of relaxation oscillators, that is there is a family of asymptotically stable limit cycles $\gamma_\delta \subset \mathbb{R}^2$ that converge in the limit $\varepsilon \rightarrow 0$ to a union of orbit segments consisting of part of the critical manifold $\{(x, y) \mid f(x, y) = 0\}$ and line segments that correspond to the fast transitions.

In a series of papers [136, 198], Somers and Kopell developed a theory to explain rapid synchronization in networks of coupled relaxation oscillators motivated by computational neuroscience. Write $z_k = (x_k, y_k)$ for the state of oscillator k which evolves according to (38) when uncoupled. The networks analyzed in [136, 198] include systems of the form

$$\begin{aligned} \varepsilon x'_k &= f(x_k, y_k) + \frac{\delta}{N} \sum_{j=1}^N h(x_j, x_k), \\ y'_k &= g(x_k, y_k), \end{aligned} \quad (\mathcal{X}_{\text{net}})$$

for $k \in \{1, \dots, N\}$ and coupling function h without specific assumptions on the coupling strength ε . The analysis [136, 198] considers the singular limit $\varepsilon \rightarrow 0$ for network interactions such that the input from one node to the other is constant on each segment of the critical manifold and evaluates the “compression” of time it takes a singular trajectory to traverse segments of the critical manifold. But even in the context of coupled neurons, other forms of network interactions h —such as pulsatile coupling—are relevant.

If both the time scale separation ε for the relaxation oscillator and the coupling strength δ are small, then the qualitative dynamics of $(\mathcal{X}_{\text{net}})$ can be understood in terms of the unified framework above. Specifically, let \mathcal{P}_{net} denote the property that we can apply a phase reduction. We obtain a system of the form (37) by dividing the fast equations $(\mathcal{X}_{\text{net}})$ by ε and setting $\eta = \delta/\varepsilon$. By fixing ε we obtain an $\eta_0(\varepsilon)$ such that \mathcal{P}_{net} holds for all $\eta < \eta_0$. Hence, there is $\delta_0(\varepsilon)$ such that \mathcal{P}_{net} holds for $\delta < \delta_0(\varepsilon)$ in $(\mathcal{X}_{\text{net}})$. This leads to the classification of the parameter space \mathcal{K} into a region (I) where \mathcal{P}_{net} holds and its complement (II). Depending on the coupling function h , we may have $\lim_{\varepsilon \rightarrow 0} \delta_0(\varepsilon) \neq 0$ (for example if $h = 0$ as mentioned above). However, for a generic interaction function one would expect $\eta_0(\varepsilon) < C$ for some constant C . In this case, we have $\lim_{\varepsilon \rightarrow 0} \delta_0(\varepsilon) = 0$ as depicted in Fig. 28.

Izhikevich [120] derived explicit expressions for the dynamics on the invariant torus in the relaxation limit. As

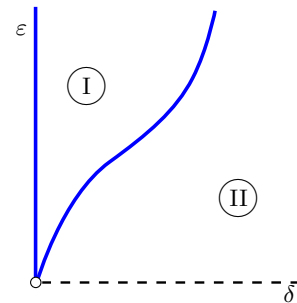


FIG. 28: The property \mathcal{P}_{net} divides the parameter space for $(\mathcal{X}_{\text{net}})$ into a region (I), where a phase reduction is possible and a region (II), where we expect a torus breakdown for a generic coupling function h . The line dividing the region is given by $\delta_0(\varepsilon)$.

noted there, these expressions only describe the doubly singular limit for paths in parameter space converging to the limit point $(\varepsilon, \delta) = (0, 0)$ that lie entirely within region (I). A first-order truncation of the phase dynamics—as commonly considered—does not describe the dynamics of the full oscillator network $(\mathcal{X}_{\text{net}})$ for all points in (I) since higher-order terms may play a nontrivial role in the dynamics [38, 41, 152].

While we focused on the interplay of small parameter in the intrinsic oscillator dynamics and the network coupling, interacting small parameters also naturally arise in different ways in networked systems. In contrast to coupled relaxation oscillators, one can also consider the case of coupled oscillators close to a Hopf bifurcation where oscillations are almost sinusoidal. Considering both small bifurcation parameter and weak coupling, one obtains explicit phase reductions [8] that can—depending on the order of the approximation—contain nonpairwise interaction terms as mentioned above. Limits involving multiple small parameters also occur if the network connections are adaptive [96]. This includes for example networks of neurons [61, 65, 166] or adaptation in epidemic networks [97]. Indeed, oscillator networks with adaptive interactions on have received renewed attention recently, whether the adaptation is slow (see e.g., [36, 132, 195]) or fast [6] relative to the oscillatory dynamics. However, there are only few approaches taking into account distinct time scales explicitly (cf. [125]) in particular when multiple small parameters interact. Thus, for adaptive networks with multiple time scales, the framework presented here may help classify the dynamics of such coupled oscillator networks.

4. COMPARISON

In Section 3, we have described a wide variety of doubly-singular limit problems arising in differential equations. Yet, from the different examples, several natural themes emerge for the future of multiple singular limit systems.

Property Types: We have seen various ways of defining properties \mathcal{P} to obtain double limits which, however, share quite surprising similarities:

- *Individual Pattern Classification:* It turned out to be extremely useful to define \mathcal{P} via important types of patterns, e.g., the number of solutions/roots of an algebraic equation in Section 2.1, the slow manifold shapes near the transcritical point as well as the oscillation patterns for the Olsen model in Section 3.1, the stochastic excitable patterns for FitzHugh–Nagumo in Section 3.2, the types of stationary patterns for MEMS in Section 3.5, and the number of bifurcation points for fast reaction PDEs in Section 3.6.
- *Phase Space Structure:* A strongly related class of properties emerges once one investigates pattern-forming properties more on a global level studying the entire phase space at once. Examples are probabilistic quantifiers such as escape probabilities in Section 3.2, the sign of the first Lyapunov exponent in Section 3.3 for oscillators with shear, or the global stability for linear PDMPs in Section 3.4.
- *Mathematical Features:* A last important class of properties has emerged corresponding to elements of proofs or mathematical properties. This includes convexity from Section 2.1, the exchange of partial derivatives in Section 2.2, the existence of a stationary distribution in Section 3.4, or the applicability of phase reduction for networks of oscillators in Section 3.7.

In view of all the preceding examples, it seems difficult to imagine that, for practical problems in singularly perturbed differential equations, there are highly useful properties that do not fit within the three classes mentioned above. In fact, we see that each class asks a different type of question, namely: How to understand individual/observed patterns? How to understand the global structure of phase space? What are the technical ingredients for proofs? Looking forward, it always seems useful directly at the start of a work on double- (or multiple-) limits to state carefully the major type of property one is interested in for dissecting the non-negative parameter cone \mathcal{K} .

Diagram Structures: Even if one has obtained a suitable partitioning of \mathcal{K} , one can now ask, comparing to other typical double limit problems, whether this partitioning via \mathcal{P} is “typical” or “common”? Quite surprisingly, a cohesive and well-founded answer to this problem is possible as many common features seem to emerge in $(\varepsilon, \delta) \rightarrow (0, 0)$ double-limit diagrams:

- *Origin Ill-Posedness:* Very frequently, it turns out that classifying the origin $(\varepsilon, \delta) = (0, 0)$ is ill-posed as \mathcal{P} is not well-defined or virtually impossible to evaluate at the origin. This situation is completely

satisfactory from an applied mathematical perspective as one has the small parameters in the problem as they are small, yet still non-zero; so we do not really lose major information if we exclude the origin in most problems.

- *Special Axes:* Another common theme is that the two axes $\{\varepsilon = 0, \delta > 0\}$ $\{\varepsilon > 0, \delta = 0\}$ have special or degenerate properties with respect to \mathcal{P} . As for the origin, we do not give up much in many cases if we discard these two axes, yet it is often these two cases where proofs can become easier. Hence, it is often a suitable strategy to understand the axes, and then aim for a perturbation, homotopy, or extension of the results to the interior of the cone \mathcal{K} .
- *Polynomial Dissection:* As expected from classical scaling law results in physics as well as from the mathematical viewpoint of singularity/regularity theory, we often find curves $\delta = \delta(\varepsilon)$ (resp. $\varepsilon = \varepsilon(\delta)$) with $\delta(0) = 0$ (resp. $\varepsilon(0) = 0$), which provide a partitioning of the cone \mathcal{K} . Indeed, local Taylor (or Hölder-type) expansions should naturally appear, and one can then classify the partitioning of \mathcal{K} via the critical powers/exponents of the leading-order terms of the curves.
- *Special Features:* Certain problems, either due to their inherent natural problem formulation or due to dynamical effects, may lead to non-polynomial or otherwise special dissection. Examples are exponential terms arising in stochastic metastability as well as for canard problems, or curves without $\varepsilon(0) = 0$ as for fast-reaction bifurcation points.

In summary, it seems clear that a complete unifying classification is impossible but in many cases a rather exhaustive description can be provided within a common framework. First, one can aim to classify the behaviour on the axis for a single limit problem. Second, one can aim to obtain a set of (polynomial) curves partitioning the interior of \mathcal{K} including the leading-order scaling exponents. Third, one aims to check whether there are any special cases occurring for the polynomial scaling or lack of connectivity of the curves to the origin; these special cases are then treated on a case-by-case basis and/or using a suitable shift or re-scaling to obtain polynomial order and/or connecting curves.

Mathematical Techniques: Another important lesson from the comparison of the different examples of doubly-singularly perturbed problems is that the analytical and numerical techniques tend to look very different at first sight. Yet, this seems to be a superficial view if one delves deeper into each methodology. There are many common themes appearing. First, numerical methods tend to become more “stiff” near singular limits, yet analytical methods become far more feasible the closer we are to the origin within \mathcal{K} . This implies that a

natural approach is to combine both approaches within \mathcal{K} by locally using analytical techniques and then extend the results beyond a small neighborhood of $(\varepsilon, \delta) = (0, 0)$ via numerical computations. Second, analytical methods are always based upon similar principles, regardless of the differential equation studied:

- *Limit equations:* In a simple limit with one parameter fixed, i.e., on the coordinate axes in the two-parameter plane, we can often obtain a reduced problem from which to start.
- *Relative scaling:* It frequently makes sense to assume the existence of a relative scaling $\varepsilon = \varepsilon(\delta)$ (resp. $\delta = \delta(\varepsilon)$), which provides again one-parameter families of sub-problems lying on curves in the interior of \mathcal{K} .
- *Desingularization:* It often makes sense via geometric desingularization such as blow-up, or just via purely algebraic scaling, to generate a more complicated differential equation, which better splits the relative scalings.
- *Regularization:* Some problems become significantly easier if another singular parameter is added, e.g., noise is well-known to regularize the dynamics in many instances. In fact, we have seen this effect for excitable systems as well as for stochastically perturbed limit cycles where a non-hyperbolic structure collapses.

In summary, also the mathematical techniques to attack very distant-looking singular perturbation problems are more deeply related than one might anticipate.

5. OUTLOOK

In this review, we have only been able to illustrate a more general framework for differential equations with multiple small parameters for certain classes of problems. It is evident that many important questions still remain. To illustrate the diversity of remaining problems, we present a few crucial questions that seem tractable within the next couple of decades:

(Q1) For many double-singular perturbations, multiple methodological approaches exist and we definitely need a better understanding how these approaches can be compared more directly in concrete double-limit test problems. This approach is very common in other mathematical disciplines, e.g., in numerical analysis, which often provides sharp and precise comparisons of algorithms, or even in classical analysis, where many problems involve the derivation of best-possible upper a-priori bounds. As a concrete example for the case of double limits, consider the case of multiple time scale stochastic problems discussed in Section 3.2. We have

shown a sample-paths approach to estimate probabilities, but alternatively one could also use a distributional approach via the Fokker-Planck equation, non-autonomous dynamics techniques such as skew-product flows, quasi-stationary distributions, matched asymptotic expansions, numerical methods, as well as many other methods to study the double limit. The same remark applies to all other examples we have discussed. A detailed discussion of the advantages and disadvantages of every method for double limits is clearly an open problem.

(Q2) For many double-limit problems, there are concrete conjectures left to be proven for certain regions in the two-parameter diagrams. A good example is the Olsen model in Section 3.1, where the case of non-classical relaxation oscillations is solved. Yet, rigorous proofs for mixed-mode/bursting-type oscillations as well as chaotic dynamics are missing although the geometry of the orbits has been illuminated well via singular limits as well as via numerics. This is actually a common theme for all the problems, i.e., even though certain scaling regimes are tractable, it is often extremely challenging to cover the entire parameter space via rigorous proofs. An excellent goal for future research could be to develop better first-principles mathematical indicators, which tell us much quicker about the difficulties of certain scaling regions. Currently, trial-and-error is still often our best approach in this regard.

(Q3) Another natural question to follow within future work is the role played by low regularity in singular-perturbation problems. An astonishing variety of small-parameter problems in differential equations are connected to trajectories, which may have low regularity. Beyond this, even the important dynamical invariant structures (such as attractors) have low regularity. One example has been presented in Section 3.3, as shear-induced chaos for stochastic differential equations is connected to relatively rough individual sample paths and simultaneously to a chaotic attractor. Since chaotic attractors often have fractal dimension, they contribute another aspect of low regularity. In more generality, the same theme also appears for chaotic deterministic switching problems or in a completely different setting in large-scale network limits, where the regularity of the finite-dimensional problem may not always transfer to the mean-field or continuum limit.

(Q4) From a numerical perspective, many crucial challenges are posed by double-limit dynamics. In fact, even very classical stiff differential equations with a single small parameter constitute a vast area already. Having two different, yet possibly

connected, singular parameters tends to make the situation much worse. It seems wise to combine analytical pre-processing, i.e., re-writing the differential equations first into the best possible numerical problem, and careful a-priori error estimates, to avoid spurious solutions. A good example of re-writing the numerical setting has been discussed in Section 3.6, where numerical continuation in the small parameters leads to well-conditioned boundary-value problems instead of quite poorly conditioned initial-value problems. It is a very worthwhile general goal to develop as many numerical methods as possible that have robustness/well-conditioning against small-parameter limits.

- (Q5) Another aspect where many open questions remain is the interplay between double limits and areas usually quite far from classical singular-limit problems for differential equations. An illustrating example are limits in coupled oscillators as discussed in Section 3.7. More generally, one can assume that the oscillators are coupled on a graph, on a simplicial complex, or a general hypergraph [13, 41]. In these cases, methods from graph theory, combinatorics, and geometry/topology are going to enter the mathematical challenge, and double-limit problems are not as classical in these areas as they are for differential equations. Yet, exploring whether it is possible to translate open questions in double-limit problems into new areas seems to be promising.
- (Q6) We have often assumed throughout this work that the studied differential equations have quite a high degree of regularity in their defining equations as this is often the most natural starting point, e.g., by invoking a more microscopic modelling approach to retain smoothness. Even in the case of SODEs with classical white noise, we have Hölder regularity in Sections 3.2 and 3.3. Only for the PDMP case in Section 3.4, we have less regularity as discontinuous jumps occur. Of course, if one allows for arbitrary degeneracy in terms of input regularity, then this leads already to very intriguing questions on the level of existence of a suitable dynamical system, even for ODEs [48, 162]. Already for ODEs the number of possibilities for bifurcations in non-smooth systems is extremely large [73, 126] and their unfoldings via multiple small parameters involving a regularization is still under active development [55, 127]. For non-smooth SDEs and PDEs, the situation will be even more complicated. In summary, identifying principles to derive universally valid and sufficiently low-dimensional double-limit problems is already challenging once regularity assumptions are relaxed.
- (Q7) The biggest, and probably even most pressing, remaining challenge is to broaden the practical applicability of double-limit results. In fact, the

steps (S1)–(S3) in the introduction naturally apply to many other problems. For example, double-limit differential equations occur in homogenization of PDEs [167], in homogenization of fast chaos [163], in rate-independent systems modeling viscoelasticity [171], in bursting oscillations in neuroscience [203], in oscillators from systems biology [170], in plasma physics [76], in mean-field analysis of particle systems [45], in stochastic optimization [46], and in fluid dynamics [99]. Of course, this list could be continued with many additional fields.

Finally, we would like to point out that our general view on double-limit problems in differential equations might also have a general impact in several respects, not only within the areas of the examples we have presented, for the questions (Q1)–(Q7), but also well beyond:

- The diagram structure, which we have utilized to summarize the main results for each case, seems to be well-adapted to the basic case of two parameters but, using suitable projections, higher-dimensional generalizations are certainly conceivable.
- Although a complete classification of all possible scaling laws in all double-limit problems seems out of reach, a classification into generic cases via an abstract universality theory, analogous to critical exponents in physics, may very well exist.
- It seems very promising to consistently reconsider double-limit problems that might have looked too challenging in the past. With a more coherent data base and a more structured classification, one might be able to search for new methods in virtually any other doubly-singular limit problem.

Acknowledgments

CK has been supported by a Lichtenberg Professorship of the VolkswagenStiftung. CK also acknowledges inspiring discussions with Grigorios A. Pavliotis regarding limit problems in differential equations, which were made possible by a TUM John von Neumann Visiting Professorship. NB has been supported by the ANR project PERISTOCH, ANR-19-CE40-0023. CB has been supported by the Institute for Advanced Study at the Technical University of Munich through a Hans Fischer fellowship and the Engineering and Physical Sciences Research Council (EPSRC) through the grant EP/T013613/1. ME has been supported by Germany's Excellence Strategy – The Berlin Mathematics Research Center MATH+ (EXC-2046/1, project ID: 390685689). CS has received funding from the European Union's Horizon 2020 research and innovation program under the Marie Skłodowska-Curie grant agreement No. 754462. Support by INdAM-GNFM is gratefully acknowledged

by CS. TH gratefully acknowledges support through SNF grant 200021 – 175728/1.

-
- [1] A. Arnaudon, A. L. De Castro, and D. D. Holm. Noise and dissipation on coadjoint orbits. *J. Nonlinear Sci.*, 28(1):91–145, 2018.
- [2] L. Arnold. *Random Dynamical Systems*. Springer, Berlin, 1998.
- [3] L. Arnold, N. Sri Namachchivaya, and K.R. Schenck-Hoppé. Toward an understanding of stochastic Hopf bifurcation: a case study. *Internat. J. Bifur. Chaos Appl. Sci. Engrg.*, 6(11):1947–1975, 1996.
- [4] S. Arrhenius. On the reaction velocity of the inversion of cane sugar by acids. *J. Phys. Chem.*, 4:226, 1889. In German. Translated and published in: Selected Readings in Chemical Kinetics, M.H. Back and K.J. Laidler (eds.), Pergamon, Oxford, 1967.
- [5] P. Ashwin and J.W. Swift. The dynamics of n weakly coupled identical oscillators. *J. Nonlinear Sci.*, 2(1):69–108, 1992.
- [6] Peter Ashwin, Christian Bick, and Camille Poignard. State-dependent effective interactions in oscillator networks through coupling functions with dead zones. *Philosophical Transactions of the Royal Society A: Mathematical, Physical and Engineering Sciences*, 377(2160):20190042, 2019.
- [7] Peter Ashwin, Stephen Coombes, and Rachel Nicks. Mathematical Frameworks for Oscillatory Network Dynamics in Neuroscience. *The Journal of Mathematical Neuroscience*, 6(1):2, 2016.
- [8] Peter Ashwin and Ana Rodrigues. Hopf normal form with S_N symmetry and reduction to systems of nonlinearly coupled phase oscillators. *Physica D*, 325:14–24, 2016.
- [9] Y. Bakhtin and Tobias H. Invariant densities for dynamical systems with random switching. *Nonlinearity*, 25(10):2937–2952, 2012.
- [10] Y. Bakhtin, T. Hurth, S.D. Lawley, and J.C. Mattingly. Singularities of invariant densities for random switching between two linear odes in 2D. *arXiv:2009.01299*, 2020.
- [11] Y. Bakhtin, T. Hurth, and J.C. Mattingly. Regularity of invariant densities for 1d-systems with random switching. *Nonlinearity*, 28:3755–3787, 2015.
- [12] M. Balde, U. Boscaïn, and P. Mason. A note on stability conditions for planar switched systems. *Internat. J. Control*, 82(10):1882–1888, 2009.
- [13] Federico Battiston, Giulia Cencetti, Iacopo Iacopini, Vito Latora, Maxime Lucas, Alice Patania, Jean-gabriel Young, and Giovanni Petri. Networks beyond pairwise interactions: Structure and dynamics. *Physics Reports*, 874:1–92, 2020.
- [14] Peter H. Baxendale and Priscilla E. Greenwood. Sustained oscillations for density dependent Markov processes. *J. Math. Biol.*, 63(3):433–457, 2011.
- [15] P.H. Baxendale. A stochastic Hopf bifurcation. *Probab. Theory Related Fields*, 99(4):581–616, 1994.
- [16] P.H. Baxendale. Lyapunov exponents and stability for the stochastic Duffing-van der Pol oscillator. In *IUTAM Symposium on Nonlinear Stochastic Dynamics*, volume 110 of *Solid Mech. Appl.*, pages 125–135. Kluwer Acad. Publ., Dordrecht, 2003.
- [17] P.H. Baxendale. Stochastic averaging and asymptotic behavior of the stochastic Duffing-van der Pol equation. *Stochastic Process. Appl.*, 113(2):235–272, 2004.
- [18] M. Benaïm. Stochastic persistence (part I). Available at <https://arxiv.org/abs/1806.08450>, 2018. preprint.
- [19] M. Benaïm, S. Le Borgne, F. Malrieu, and P.-A. Zitt. On the stability of planar randomly switched systems. *Ann. Appl. Probab.*, 24(1):292–311, 2014.
- [20] M. Benaïm, S. Le Borgne, F. Malrieu, and P.-A. Zitt. Qualitative properties of certain piecewise deterministic Markov processes. *Ann. Inst. Henri Poincaré Probab. Stat.*, 51(3):1040–1075, 2015.
- [21] Michel Benaïm, Tobias Hurth, and Edouard Strickler. A user-friendly condition for exponential ergodicity in randomly switched environments. *Electron. Commun. Probab.*, 23:1–12, 2018.
- [22] Michel Benaïm, Stéphane Le Borgne, Florent Malrieu, and Pierre-André Zitt. Quantitative ergodicity for some switched dynamical systems. *Electron. Commun. Probab.*, 17:no. 56, 14, 2012.
- [23] Michel Benaïm and Edouard Strickler. Random switching between vector fields having a common zero. *Ann. Appl. Probab.*, 29(1):326–375, 2019.
- [24] Michel Benaïm and Claude Lobry. Lotka–volterra with randomly fluctuating environments or “how switching between beneficial environments can make survival harder”. *Ann. Appl. Probab.*, 26(6):3754–3785, 12 2016.
- [25] C.M. Bender and S.A. Orszag. *Asymptotic Methods and Perturbation Theory*. Springer, 1999.
- [26] E. Benoît, J.L. Callot, F. Diener, and M. Diener. Chasse au canards. *Collect. Math.*, 31:37–119, 1981.
- [27] A. Bensoussan, J.-L. Lions, and G. Papanicolaou. *Asymptotic analysis for periodic structures*. Chelsea, 2011.
- [28] C. Berardo, S. Geritz, M. Gyllenberg, and G. Raul. Co-evolution of the reckless prey and the patient predator. *J. Math. Biol.*, 2021.
- [29] N. Berglund and B. Gentz. Pathwise description of dynamic pitchfork bifurcations with additive noise. *Probab. Theory Rel.*, 122(3):341–388, 2002.
- [30] N. Berglund and B. Gentz. A sample-paths approach to noise-induced synchronization: Stochastic resonance in a double-well potential. *Ann. Appl. Probab.*, 12:1419–1470, 2002.
- [31] N. Berglund and B. Gentz. Geometric singular perturbation theory for stochastic differential equations. *J. Differ. Equations*, 191:1–54, 2003.
- [32] N. Berglund and B. Gentz. *Noise-induced phenomena in slow-fast dynamical systems. A sample-paths approach*. Probability and its Applications. Springer-Verlag, London, 2006.
- [33] N. Berglund, B. Gentz, and C. Kuehn. Hunting French ducks in a noisy environment. *J. Differ. Equations*, 252(9):4786–4841, 2012.
- [34] N. Berglund, B. Gentz, and C. Kuehn. From random Poincaré maps to stochastic mixed-mode-oscillation patterns. *J. Dyn. Differ. Equ.*, 27(1):83–136, 2015.
- [35] N. Berglund and D. Landon. Mixed-mode oscillations

- tions and interspike interval statistics in the stochastic FitzHugh-Nagumo model. *Nonlinearity*, 25(8):2303–2335, 2012.
- [36] R. Berner, E. Schöll, and S. Yanchuk. Multiclusters in networks of adaptively coupled phase oscillators. *SIAM J. Appl. Dyn. Syst.*, 18(4):2227–2266, 2019.
- [37] G. Beutler. *Methods of Celestial Mechanics (volume I): physical, mathematical, and numerical principles*. Springer, 2004.
- [38] C. Bick, P. Ashwin, and A. Rodrigues. Chaos in generically coupled phase oscillator networks with nonpairwise interactions. *Chaos*, 26(9):094814, 2016.
- [39] C. Bick, M. Timme, D. Paulikat, D. Rathlev, and P. Ashwin. Chaos in symmetric phase oscillator networks. *Phys. Rev. Lett.*, 107(24):244101, 2011.
- [40] Christian Bick, Marc Goodfellow, Carlo R. Laing, and Erik A. Martens. Understanding the dynamics of biological and neural oscillator networks through exact mean-field reductions: a review. *The Journal of Mathematical Neuroscience*, 10(1):9, 2020.
- [41] Christian Bick, Elizabeth Gross, Heather A. Harrington, and Michael T. Schaub. What are higher-order networks? *arXiv:2104.11329*, apr 2021.
- [42] N. Blackbeard, H. Erzgräber, and S. Wiczorek. Shear-induced bifurcations and chaos in models of three coupled lasers. *SIAM J. Appl. Dyn. Syst.*, 10(2):469–509, 2011.
- [43] A. Blumenthal, J. Xue, and L.-S. Young. Lyapunov exponents for random perturbations of some area-preserving maps including the standard map. *Ann. of Math. (2)*, 185(1):285–310, 2017.
- [44] A. Blumenthal, J. Xue, and L.-S. Young. Lyapunov exponents and correlation decay for random perturbations of some prototypical 2D maps. *Comm. Math. Phys.*, 359(1):347–373, 2018.
- [45] M. Bodnar and J.J.L. Velázquez. An integro-differential equation arising as a limit of individual cell-based models. *J. Differen. Equat.*, 222(2):341–380, 2006.
- [46] V.S. Borkar and S.K. Mitter. A strong approximation theorem for stochastic recursive algorithms. *J. Optim. Theor. Appl.*, 100(3):499–513, 1999.
- [47] Peter Borowski, Rachel Kuske, Yue-Xian Li, and Juan Luis Cabrera. Characterizing mixed mode oscillations shaped by noise and bifurcation structure. *Chaos*, 20(4):043117, 2010.
- [48] E. Bossolini, M. Brøns, and K.U. Kristiansen. A stiction oscillator with canards: on piecewise smooth nonuniqueness and its resolution by regularization using geometric singular perturbation theory. *SIAM Rev.*, 62(4):869–897, 2020.
- [49] D. Bothe and D. Hilhorst. A reaction–diffusion system with fast reversible reaction. *J. Math. Anal. Appl.*, 286(1):125–135, 2003.
- [50] D. Bothe and M. Pierre. The instantaneous limit for reaction-diffusion systems with a fast irreversible reaction. *Discrete Contin. Dyn. Syst. Ser. S*, 5(1):49, 2012.
- [51] H. Boudjellaba and T. Sari. Dynamic transcritical bifurcations in a class of slow-fast predator-prey models. *J. Diff. Eq.*, 246:2205–2225, 2009.
- [52] M. Breden and M. Engel. Computer-assisted proof of shear-induced chaos in stochastically perturbed Hopf systems. *arXiv:2101.01491*, pages 1–39, 2020.
- [53] M. Breden, C. Kuehn, and C. Soresina. On the influence of cross-diffusion in pattern formation. *J. Comput. Dyn.*, 8(2):213–240, 2021.
- [54] E. Brocchieri, L. Corrias, H. Dietert, and Y.-J. Kim. Evolution of dietary diversity and a starvation driven cross-diffusion system as its singular limit. *arXiv preprint arXiv:2011.10304*, 2020.
- [55] C.A. Buzzi, P.R. da Silva, and M.A. Teixeira. A singular approach to discontinuous vector fields on the plane. *J. Diff. Eq.*, 231:633–655, 2006.
- [56] P.T. Cardin and M.A. Teixeira. Fenichel theory for multiple time scale singular perturbation problems. *SIAM J. Appl. Dyn. Syst.*, 16(3):1425–1452, 2017.
- [57] J. Chen and R.E. O’Malley, Jr. On the asymptotic solution of a two-parameter boundary value problem of chemical reactor theory. *SIAM J. Appl. Math.*, 26(4):717–729, 1974.
- [58] B. Cloez and M. Hairer. Exponential ergodicity for Markov processes with random switching. *Bernoulli*, 21:505–536, 2015.
- [59] F. Conforto and L. Desvillettes. Rigorous passage to the limit in a system of reaction–diffusion equations towards a system including cross diffusions. *Commun. Math. Sci.*, 12(3):457–472, 2014.
- [60] F. Conforto, L. Desvillettes, and C. Soresina. About reaction–diffusion systems involving the Holling-type II and the Beddington–DeAngelis functional responses for predator–prey models. *Nonlinear Differ. Equ. Appl.*, 25(3):24, 2018.
- [61] S. F. Cooke and T. V. P. Bliss. Plasticity in the human central nervous system. *Brain*, 129(7):1659–1673, 2006.
- [62] Hans Crauel and Franco Flandoli. Additive noise destroys a pitchfork bifurcation. *J. Dynam. Differential Equations*, 10(2):259–274, 1998.
- [63] Dawid Czapla, Katarzyna Horbacz, and Hanna Wojewódka-Ściażko. On absolute continuity of invariant measures associated with a piecewise-deterministic Markov processes with random switching between flows. Available at <https://arxiv.org/abs/2004.06798>, 2021.
- [64] G. Da Prato and J. Zabczyk. *Ergodicity for infinite-dimensional systems*, volume 229 of *London Mathematical Society Lecture Note Series*. Cambridge University Press, Cambridge, 1996.
- [65] Yang Dan and Mu-ming Poo. Spike Timing-Dependent Plasticity of Neural Circuits. *Neuron*, 44(1):23–30, 2004.
- [66] M.H.A. Davis. Piecewise-deterministic Markov processes: a general class of nondiffusion stochastic models. *J. Roy. Statist. Soc. Ser. B*, 46(3):353–388, 1984. With discussion.
- [67] H. Degn, L.F. Olsen, and J.W. Perram. Bistability, oscillation, and chaos in an enzyme reaction. *Ann. N. Y. Acad. Sci.*, 316(1):623–637, 1979.
- [68] M. Desroches, J. Guckenheimer, C. Kuehn, B. Krauskopf, H. Osinga, and M. Wechselberger. Mixed-mode oscillations with multiple time scales. *SIAM Rev.*, 54(2):211–288, 2012.
- [69] M. Desroches, B. Krauskopf, and H.M. Osinga. The geometry of mixed-mode oscillations in the Olsen model for the peroxidase-oxidase reaction. *DCDS-S*, 2(4):807–827, 2009.
- [70] L. Desvillettes and C. Soresina. Non-triangular cross-diffusion systems with predator–prey reaction terms. *Ric. Mat.*, 68(1):295–314, 2019.
- [71] L. Desvillettes and A. Trescases. New results for triangular reaction cross diffusion system. *J. Math. Anal.*

- Appl.*, 430(1):32–59, 2015.
- [72] L. DeVille, N. Sri Namachivaya, and Z. Rapti. Stability of a stochastic two-dimensional non-Hamiltonian system. *SIAM J. Appl. Math.*, 71(4):1458–1475, 2011.
- [73] M. di Bernardo, C.J. Budd, A.R. Champneys, and P. Kowalczyk. *Piecewise-smooth Dynamical Systems*, volume 163 of *Applied Mathematical Sciences*. Springer, 2008.
- [74] Susanne Ditlevsen and Priscilla Greenwood. The Morris-Lecar neuron model embeds a leaky integrate-and-fire model. *Journal of Mathematical Biology*, 67(2):239–259, 2013.
- [75] T.S. Doan, M. Engel, J.S.W. Lamb, and M. Rasmussen. Hopf bifurcation with additive noise. *Nonlinearity*, 31(10):4567–4601, 2018.
- [76] D. Donatelli and P. Marcati. A quasineutral type limit for the Navier-Stokes-Poisson system with large data. *Nonlinearity*, 21(1):135–148, 2008.
- [77] F. Dumortier. Techniques in the theory of local bifurcations: blow-up, normal forms, nilpotent bifurcations, singular perturbations. In *Bifurcations and Periodic Orbits of Vector Fields (Montreal, PQ, 1992)*, volume 408 of *NATO Adv. Sci. Inst. Ser. C Math. Phys. Sci.*, pages 19–73. Kluwer Acad. Publ., Dordrecht, 1993.
- [78] F. Dumortier and R. Roussarie. Canard cycles and center manifolds. *Mem. Amer. Math. Soc.*, 121(577):x+100, 1996.
- [79] J. Eliaš, D. Hilhorst, M. Mimura, and Y. Morita. Singular limit for a reaction-diffusion-ode system in a neolithic transition model. *submitted*, 2020.
- [80] J. Eliaš, M.H. Kabir, and M. Mimura. On the well-posedness of a dispersal model for farmers and hunter-gatherers in the Neolithic transition. *Mathematical Models and Methods in Applied Sciences*, 28(02):195–222, 2018.
- [81] M. Engel, M.A. Gkogkas, and C. Kuehn. Homogenization of coupled fast-slow systems via intermediate stochastic regularization. *J. Stat. Phys.*, April 2021. [Online]. doi: <https://doi.org/10.1007/s10955-021-02765-7>.
- [82] M. Engel and C. Kuehn. Discretized fast-slow systems near transcritical singularities. *Nonlinearity*, 32(7):2365–2391, 2019.
- [83] M. Engel, J.S.W. Lamb, and M. Rasmussen. Bifurcation analysis of a stochastically driven limit cycle. *Comm. Math. Phys.*, 365(3):935–942, 2019.
- [84] M. Engel, J.S.W. Lamb, and M. Rasmussen. Conditioned Lyapunov exponents for random dynamical systems. *Trans. Amer. Math. Soc.*, 372(9):6343–6370, 2019.
- [85] A. Faggionato, D. Gabrielli, and M. Ribezzi Crivellari. Non-equilibrium thermodynamics of piecewise deterministic Markov processes. *J. Stat. Phys.*, 137(2):259–304, 2009.
- [86] A. Faggionato, D. Gabrielli, and M. Ribezzi Crivellari. Averaging and large deviation principles for fully-coupled piecewise deterministic Markov processes and applications to molecular motors. *Markov Process. Relat.*, 16:497–548, 2010.
- [87] D. Faranda, Y. Sato, B. Saint-Michel, C. Wiertel, V. Padilla, B. Dubrulle, and F. Daviaud. Stochastic chaos in a turbulent swirling flow. *Phys. Rev. Lett.*, 119:014502, Jul 2017.
- [88] N. Fenichel. Geometric singular perturbation theory for ordinary differential equations. *J. Differential Equat.*, 31:53–98, 1979.
- [89] R. FitzHugh. Impulses and physiological states in theoretical models of nerve membrane. *Biophys. J.*, 1(6):445–466, 1961.
- [90] M.I. Freidlin. Quasi-deterministic approximation, metastability and stochastic resonance. *Physica D*, 137:333–352, 2000.
- [91] M.I. Freidlin and A.D. Wentzell. *Random perturbations of dynamical systems*, volume 260 of *Grundlehren der Mathematischen Wissenschaften [Fundamental Principles of Mathematical Sciences]*. Springer-Verlag, New York, second edition, 1998. Translated from the 1979 Russian original by Joseph Szücs.
- [92] D.D. Freund. A note on Kaplan limits and double asymptotics. *Proc. Amer. Math. Soc.*, 35(2):464–470, 1972.
- [93] S. Geritz and M. Gyllenberg. A mechanistic derivation of the DeAngelis–Beddington functional response. *J. Theor. Biol.*, 314:106–108, 2012.
- [94] J.M. Ginoux and C. Letellier. Van der Pol and the history of relaxation oscillations: Toward the emergence of a concept. *Chaos*, 22(2):023120, 2012.
- [95] J.L. Gracia, E. O’Riordan, and M.L. Pickett. A parameter robust second order numerical method for a singularly perturbed two-parameter problem. *Appl. Numer. Math.*, 56(7):962–980, 2006.
- [96] Thilo Gross and Bernd Blasius. Adaptive coevolutionary networks: a review. *Journal of The Royal Society Interface*, 5(20):259–271, 2008.
- [97] Thilo Gross, Carlos J. Dommar D’Lima, and Bernd Blasius. Epidemic Dynamics on an Adaptive Network. *Physical Review Letters*, 96(20):208701, 2006.
- [98] J. Guckenheimer, M. Wechselberger, and L.-S. Young. Chaotic attractors of relaxation oscillations. *Nonlinearity*, 19:701–720, 2006.
- [99] W. Schneider H. Steinrück and W. Grillhofer. A multiple scales analysis of the undular hydraulic jump in turbulent open channel flow. *Fluid Dyn. Res.*, 33(1):41–55, 2003.
- [100] R. Haberman. Slowly varying jump and transition phenomena associated with algebraic bifurcation problems. *SIAM J. Appl. Math.*, 37(1):69–106, 1979.
- [101] R. Haiduc. Horseshoes in the forced van der Pol system. *Nonlinearity*, 22:213–237, 2009.
- [102] F. Henneke and B.Q. Tang. Fast reaction limit of a volume–surface reaction–diffusion system towards a heat equation with dynamical boundary conditions. *Asymptotic Analysis*, 98(4):325–339, 2016.
- [103] D. Herceg. Fourth-order finite-difference method for boundary value problems with two small parameters. *Appl. Math. Comput.*, 218(2):616–627, 2011.
- [104] D. Hilhorst, J.R. King, and M. Röger. Mathematical analysis of a model describing the invasion of bacteria in burn wounds. *Nonlinear Anal. Theory Methods Appl.*, 66(5):1118–1140, 2007.
- [105] D. Hilhorst, M. Mimura, and H. Ninomiya. Fast reaction limit of competition-diffusion systems. *Handbook of differential equations: evolutionary equations*, 5:105–168, 2009.
- [106] P. Hitzchenko and G.S. Medvedev. Bursting oscillations induced by small noise. *SIAM J. Appl. Math.*, 69:1359–1392, 2009.
- [107] M.H. Holmes. *Introduction to Perturbation Methods*. Springer, 1995.

- [108] P. Holmes. Poincaré, celestial mechanics, dynamical-systems theory and “chaos”. *Phys. Rep.*, 193(3):137–163, 1990.
- [109] F.C. Hoppensteadt and E.M. Izhikevich. *Weakly Connected Neural Networks*, volume 126 of *Applied Mathematical Sciences*. Springer, New York, NY, 1997.
- [110] W. Horsthemke and R. Lefever. *Noise-Induced Transitions*. Springer, 2006.
- [111] D. W. Hughes and M. R. E. Proctor. Chaos and the effect of noise in a model of three-wave model coupling. *Phys. D*, 46(2):163–176, 1990.
- [112] D. W. Hughes and M. R. E. Proctor. A low-order model of the shear instability of convection: chaos and the effect of noise. *Nonlinearity*, 3(1):127–153, 1990.
- [113] G. Huisman and R.J. De Boer. A formal derivation of the Beddington functional response. *J. Theor. Biol.*, 185(3):389–400, 1997.
- [114] T. Hurth and C. Kuehn. Random switching near bifurcations. *Stoch. Dyn.*, 20(2):2050008, 28, 2020.
- [115] Christiaan Huygens. *Oeuvres complètes de Christiaan Huygens. Publiées par la Société hollandaise des sciences*. M. Nijhoff, La Haye, 1888.
- [116] M. Iida, M. Mimura, and H. Ninomiya. Diffusion, cross-diffusion and competitive interaction. *J. Math. Biol.*, 53(4):617–641, 2006.
- [117] P. Imkeller and C. Lederer. An explicit description of the Lyapunov exponents of the noisy damped harmonic oscillator. *Dynamics and Stability of Systems*, 14(4):385–405, 1999.
- [118] P. Imkeller and C. Lederer. Some formulas for Lyapunov exponents and rotation numbers in two dimensions and the stability of the harmonic oscillator and the inverted pendulum. *Dynam. Syst.*, 16(1):29–61, 2001.
- [119] A. Iuorio, N. Popović, and P. Szmolyan. Singular perturbation analysis of a regularized MEMS model. *SIAM J. Appl. Dyn. Syst.*, 18(2):661–708, jan 2019.
- [120] E.M. Izhikevich. Phase equations for relaxation oscillators. *SIAM J. Appl. Math.*, 60(5):1789–1804, 2000.
- [121] H. Izuhara and M. Mimura. Reaction–diffusion system approximation to the cross-diffusion competition system. *Hiroshima Math. J.*, 38(2):315–347, 2008.
- [122] E.M. De Jager and J. Furu. *The Theory of Singular Perturbations*. North-Holland, 1996.
- [123] Kalvis M. Jansons and G. D. Lythe. Stochastic calculus: application to dynamic bifurcations and threshold crossings. *J. Statist. Phys.*, 90(1–2):227–251, 1998.
- [124] H. Jardón-Kojakhmetov, C. Kuehn, M. Sensi, and A. Pugliese. A geometric analysis of the SIR, SIRS and SIRWS epidemiological models. *Nonl. Anal.: Real World Appl.*, 58:103220, 2021.
- [125] Hildeberto Jardón-Kojakhmetov and Christian Kuehn. On Fast-Slow Consensus Networks with a Dynamic Weight. *Journal of Nonlinear Science*, 30(6):2737–2786, 2020.
- [126] M.R. Jeffrey. *Hidden Dynamics: The Mathematics of Switches, Decisions and Other Discontinuous Behaviour*. Springer, 2018.
- [127] S. Jelbart, K.U. Kristiansen, and M. Wechselberger. Singularly perturbed boundary-equilibrium bifurcations. *arXiv:2103.09613*, pages 1–43, 2021.
- [128] C.K.R.T. Jones. Geometric singular perturbation theory. In *Dynamical Systems (Montecatini Terme, 1994)*, volume 1609 of *Lect. Notes Math.*, pages 44–118. Springer, 1995.
- [129] Yuri Kabanov and Sergei Pergamenschikov. *Two-scale stochastic systems*, volume 49 of *Applications of Mathematics (New York)*. Springer-Verlag, Berlin, 2003. Asymptotic analysis and control, Stochastic Modelling and Applied Probability.
- [130] M.K. Kadalbajoo and A.S. Yadaw. B-Spline collocation method for a two-parameter singularly perturbed convection–diffusion boundary value problems. *Appl. Math. Comput.*, 201(1-2):504–513, 2008.
- [131] T.J. Kaper. An introduction to geometric methods and dynamical systems theory for singular perturbation problems. analyzing multiscale phenomena using singular perturbation methods. In J. Cronin and R.E. O’Malley, editors, *Analyzing Multiscale Phenomena Using Singular Perturbation Methods*, pages 85–131. Springer, 1999.
- [132] Dmitry V. Kasatkin, Vladimir V. Klinshov, and Vladimir I. Nekorkin. Itinerant chimeras in an adaptive network of pulse-coupled oscillators. *Physical Review E*, 99(2):022203, 2019.
- [133] J. Kevorkian and J.D. Cole. *Multiple Scale and Singular Perturbation Methods*. Springer, 1996.
- [134] R.Z. Khas’minskii. Necessary and sufficient conditions for the asymptotic stability of linear stochastic systems. *Theory Probab. Appl.*, 12(1):144–147, 1967.
- [135] B.W. Kooi, J.C. Poggiale, P. Auger, and S.A.L.M. Kooijman. Aggregation methods in food chains with nutrient recycling. *Ecol. Model.*, 157(1):69–86, 2002.
- [136] N. Kopell and D. Somers. Anti-phase solutions in relaxation oscillators coupled through excitatory interactions. *J. Math. Biol.*, 33(3):261–280, 1995.
- [137] I. Kosiuk and P. Szmolyan. Scaling in singular perturbation problems: Blowing up a relaxation oscillator. *SIAM J. Appl. Dyn. Syst.*, 10(4):1307–1343, 2011.
- [138] Efstratios K. Kosmidis and K. Pakdaman. An analysis of the reliability phenomenon in the FitzHugh–Nagumo model. *J. Comput. Neuroscience*, 14:5–22, 2003.
- [139] M. Krupa, N. Popovic, and N. Kopell. Mixed-mode oscillations in three time-scale systems: A prototypical example. *SIAM J. Appl. Dyn. Syst.*, 7(2):361–420, 2008.
- [140] M. Krupa, N. Popovic, N. Kopell, and H.G. Rotstein. Mixed-mode oscillations in a three time-scale model for the dopaminergic neuron. *Chaos*, 18:015106, 2008.
- [141] M. Krupa and P. Szmolyan. Extending geometric singular perturbation theory to nonhyperbolic points—fold and canard points in two dimensions. *SIAM J. Math. Anal.*, 33(2):286–314, 2001.
- [142] M. Krupa and P. Szmolyan. Extending slow manifolds near transcritical and pitchfork singularities. *Nonlinearity*, 14:1473–1491, 2001.
- [143] C. Kuehn. Normal hyperbolicity and unbounded critical manifolds. *Nonlinearity*, 27(6):1351–1366, 2014.
- [144] C. Kuehn. The curse of instability. *Complexity*, 20(6):9–14, 2015.
- [145] C. Kuehn. *Multiple Time Scale Dynamics*. Springer, 2015.
- [146] C. Kuehn and C. Soresina. Numerical continuation for a fast-reaction system and its cross-diffusion limit. *SN Partial Differ. Equ. Appl.*, 1:7, 2020.
- [147] C. Kuehn and P. Szmolyan. Multiscale geometry of the Olsen model and non-classical relaxation oscillations. *J. Nonlinear Sci.*, 25(3):583–629, 2015.
- [148] R. Kuske. Probability densities for noisy delay bifurcations. *J. Statist. Phys.*, 96(3–4):797–816, 1999.

- [149] S.D. Lawley, J.C. Mattingly, and M.C. Reed. Sensitivity to switching rates in stochastically switched ODEs. *Commun. Math. Sci.*, 12(7):1343–1352, 2014.
- [150] Sean D. Lawley, Jonathan C. Mattingly, and Michael C. Reed. Stochastic switching in infinite dimensions with applications to random parabolic PDE. *SIAM J. Math. Anal.*, 47(4):3035–3063, 2015.
- [151] O. Lehtinen and S.A.H. Geritz. Cyclic prey evolution with cannibalistic predators. *J. Theor. Biol.*, 479:1–13, 2019.
- [152] I. León and D. Pazó. Phase reduction beyond the first order: The case of the mean-field complex Ginzburg–Landau equation. *Phys. Rev. E*, 100(1):012211, 2019.
- [153] Dan Li, Shengqiang Liu, and Jing’an Cui. Threshold dynamics and ergodicity of an sirs epidemic model with markovian switching. *Journal of Differential Equations*, 263(12):8873 – 8915, 2017.
- [154] Dan Li and Hui Wan. Coexistence and exclusion of competitive Kolmogorov systems with semi-Markovian switching. *Discrete and Continuous Dynamical Systems*, 41(9):4145–4183, 2021.
- [155] K.K. Lin, E. Shea-Brown, and L.-S. Young. Reliability of coupled oscillators. *J. Nonlinear Sci.*, 19(5):497–545, 2009.
- [156] K.K. Lin and L.-S. Young. Shear-induced chaos. *Nonlinearity*, 21:899–922, 2008.
- [157] K.K. Lin and L.-S. Young. Dynamics of periodically kicked oscillators. *J. Fixed Point Theory Appl.*, 7(2):291–312, 2010.
- [158] B. Lindner, J. Garcia-Ojalvo, A. Neiman, and L. Schimansky-Geier. Effects of noise in excitable systems. *Physics Reports*, 392:321–424, 2004.
- [159] Benjamin Lindner and Lutz Schimansky-Geier. Analytical approach to the stochastic FitzHugh-Nagumo system and coherence resonance. *Physical Review E*, 60(6):7270–7276, 1999.
- [160] A.E. Lindsay, J. Lega, and K.B. Glasner. Regularized model of post-touchdown configurations in electrostatic MEMS: Equilibrium analysis. *Physica D*, 280:95–108, 2014.
- [161] E. Löcherbach. Absolute continuity of the invariant measure in piecewise deterministic Markov processes having degenerate jumps. *Stochastic Process. Appl.*, 128(6):1797–1829, 2018.
- [162] I.P. Longo, S. Novo, and R. Obaya. Weak topologies for Carathéodory differential equations: continuous dependence, exponential dichotomy and attractors. *J. Dyn. Diff. Eq.*, 31(3):1617–1651, 2019.
- [163] M. Engel M. Gkogkas and C. Kuehn. Homogenization of fully-coupled chaotic fast-slow systems via intermediate stochastic regularization. *arXiv:2003.11297*, pages 1–29, 2020.
- [164] Florent Malrieu and Tran Hoa Phu. Lotka-Volterra with randomly fluctuating environments: a full description. Available at <https://arxiv.org/abs/1607.04395>, 2018.
- [165] Florent Malrieu and Pierre-André Zitt. On the persistence regime for lotka-volterra in randomly fluctuating environments. *ALEA, Lat. Am. J. Probab. Math. Stat.*, 14:733–749, 2017.
- [166] Henry Markram, Wulfram Gerstner, and Per Jesper Sjöström. A history of spike-timing-dependent plasticity. *Frontiers in Synaptic Neuroscience*, 3:4, 2011.
- [167] G. Menon. Gradient systems with wiggly energies and related averaging problems. *Arch. Rat. Mech. Anal.*, 162(3):193–246, 2002.
- [168] J.A. Metz and O. Diekmann. *The dynamics of physiologically structured populations*, volume 68. Springer, 2014.
- [169] R.E. Meyer. On the approximation of double limits by single limits and the Kaplun extension theorem. *J. Inst. Math. Appl.*, 3:245–249, 1967.
- [170] Z. Miao, N. Popović, and P. Szmolyan. Oscillations in a cAMP signalling model for cell aggregation - a geometric analysis. *J. Math. Anal. Appl.*, 483(1):123577, 2020.
- [171] A. Mielke and L. Truskinovsky. From discrete viscoelasticity to continuum rate-independent plasticity: rigorous results. *Arch. Rat. Mech. Anal.*, 203(2):577–619, 2012.
- [172] E.F. Mishchenko and N.Kh. Rozov. *Differential Equations with Small Parameters and Relaxation Oscillations (translated from Russian)*. Plenum Press, 1980.
- [173] C.B. Muratov and E. Vanden-Eijnden. Noise-induced mixed-mode oscillations in a relaxation oscillator near the onset of a limit cycle. *Chaos*, 18:015111, 2008.
- [174] E. Musoke, B. Krauskopf, and H.M. Osinga. A surface of heteroclinic connections between two saddle slow manifolds in the Olsen model. *Int. J. Bif. Chaos*, 30(16):2030048, 2020.
- [175] J. Nagumo, S. Arimoto, and S. Yoshizawa. An active pulse transmission line simulating nerve axon. *Proceedings of the IRE*, 50(10):2061–2070, 1962.
- [176] H. Nakao. Phase reduction approach to synchronisation of nonlinear oscillators. *Contemp. Phys.*, 57(2):188–214, 2016.
- [177] A.H. Nayfeh. *Perturbation Methods*. Wiley, 2004.
- [178] L.F. Olsen. An enzyme reaction with a strange attractor. *Phys. Lett. A*, 94(9):454–457, 1983.
- [179] R.E. O’Malley. Two-parameter singular perturbation problems for second-order equations. *J. Math. Mech.*, 16(10):1143–1164, 1967.
- [180] R.E. O’Malley. On initial value problems for nonlinear systems of differential equations with two small parameters. *Arch. Rat. Mech. Anal.*, 40(3):209–222, 1971.
- [181] R.E. O’Malley. Singular perturbation theory: a viscous flow out of Göttingen. *Ann. Rev. Fluid Mech.*, 42:1–17, 2010.
- [182] R.E. O’Malley. *Historical Developments in Singular Perturbations*. Springer, 2014.
- [183] R.E. O’Malley Jr. Singular perturbations of boundary value problems for linear ordinary differential equations involving two parameters. *J. Math. Anal. Appl.*, 19(2):291–308, 1967.
- [184] R.E. O’Malley Jr. *Introduction to singular perturbations*. Academic Press, 1974.
- [185] W. Ott and M. Stenlund. From limit cycles to strange attractors. *Commun. Math. Phys.*, 296(1):215–249, 2010.
- [186] G.A. Pavliotis and A.M. Stuart. *Multiscale Methods: Averaging and Homogenization*. Springer, 2008.
- [187] B. Pietras and A. Daffertshofer. Network dynamics of coupled oscillators and phase reduction techniques. *Phys. Rep.*, 819:1–105, 2019.
- [188] Arkady Pikovsky, Michael Rosenblum, and Jürgen Kurths. *Synchronization: A Universal Concept in Nonlinear Sciences*. Cambridge University Press, 2003.
- [189] H. Poincaré. Mémoires et observations. Sur certaines solutions particulières du problème des trois corps. *Bulletin Astronomique*, I(1):65–74, 1884.

- [190] N. Popović and P. Szmolyan. A geometric analysis of the Lagerstrom model problem. *J. Differential Equations*, 199(2):290–325, 2004.
- [191] L. Prandtl. Über Flüssigkeiten bei sehr kleiner Reibung. In *Verh. III - International Math. Kongress*, pages 484–491. Teubner, 1905.
- [192] H.G. Roos and Z. Uzelac. The SDFEM for a convection-diffusion problem with two small parameters. *Comput. Methods Appl. Math.*, 3(3):443–458, 2003.
- [193] J.A. Sanders, F. Verhulst, and J. Murdock. *Averaging Methods in Nonlinear Dynamical Systems*. Springer, 2007.
- [194] K. R. Schenk-Hoppé. Bifurcation scenarios of the noisy Duffing-van der Pol oscillator. *Nonlinear Dynam.*, 11(3):255–274, 1996.
- [195] Philip Seliger, Stephen C. Young, and Lev S. Tsimring. Plasticity and learning in a network of coupled phase oscillators. *Physical Review E*, 65(4):041906, 2002.
- [196] N. Shigesada, K. Kawasaki, and E. Teramoto. Spatial segregation of interacting species. *J. Theor. Biol.*, 79(1):83–99, 1979.
- [197] D. W. J. Simpson and R. Kuske. Mixed-mode oscillations in a stochastic, piecewise-linear system. *Physica D*, 240:1189–1198, 2011.
- [198] D. Somers and N. Kopell. Rapid synchronization through fast threshold modulation. *Biol. Cybern.*, 68(5):393–407, 1993.
- [199] N. G. Stocks, R. Manella, and P. V. E. McClintock. Influence of random fluctuations on delayed bifurcations: The case of additive white noise. *Phys. Rev. A*, 40:5361–5369, 1989.
- [200] Edouard Strickler. Randomly switched vector fields sharing a zero on a common invariant face. *Stoch. Dyn.*, 21(2):2150007, 20, 2021.
- [201] S.H. Strogatz. *Sync: The Emerging Science of Spontaneous Order*. Penguin, 2004.
- [202] J. B. Swift, P. C. Hohenberg, and Guenter Ahlers. Stochastic Landau equation with time-dependent drift. *Phys. Rev. A*, 43:6572–6580, 1991.
- [203] W. Teka, J. Tabak, and R. Bertram. The relationship between two fast/slow analysis techniques for bursting oscillations. *Chaos*, 22:043117, 2012.
- [204] A.N. Tihonov. Systems of differential equations containing small parameters in the derivatives. *Mat. Sbornik N. S.*, 31:575–586, 1952.
- [205] Henry C. Tuckwell. *Stochastic Processes in the Neurosciences*. SIAM, Philadelphia, PA, 1989.
- [206] S. Valarmathi and N. Ramanujam. Computational methods for solving two-parameter singularly perturbed boundary value problems for second-order ordinary differential equations. *Appl. Math. Comput.*, 136(2-3):415–441, 2003.
- [207] B. van der Pol. On relaxation oscillations. *Philos. Mag.*, 7:978–992, 1926.
- [208] M. van Dyke. *Perturbation Methods in Fluid Mechanics*. Academic Press, 1964.
- [209] F. Verhulst. *Methods and Applications of Singular Perturbations: Boundary Layers and Multiple Timescale Dynamics*. Springer, 2005.
- [210] R. Vulcanović. A higher-order scheme for quasilinear boundary value problems with two small parameters. *Computing*, 67(4):287–303, 2001.
- [211] Q. Wang and L.-S. Young. From invariant curves to strange attractors. *Commun. Math. Phys.*, 225(2):275–304, 2002.
- [212] Q. Wang and L.-S. Young. Strange attractors in periodically-kicked limit cycles and Hopf bifurcations. *Commun. Math. Phys.*, 240(3):509–529, 2003.
- [213] W. Wasow. *Asymptotic Expansions for Ordinary Differential Equations*. Dover, 2002.
- [214] M. Wechselberger. *Geometric Singular Perturbation Theory beyond the Standard Form*. Springer, 2020.
- [215] K. C. A. Wedgwood, K. K. Lin, R. Thul, and S. Coombes. Phase-amplitude descriptions of neural oscillator models. *J. Math. Neurosci.*, 3, 2013.
- [216] S. Wicczorek. Stochastic bifurcation in noise-driven lasers and Hopf oscillators. *Phys. Rev. E*, 79:1–10, 2009.
- [217] G. George Yin and Chao Zhu. *Hybrid switching diffusions*, volume 63 of *Stochastic Modelling and Applied Probability*. Springer, New York, 2010. Properties and applications.
- [218] L.-S. Young. Chaotic phenomena in three settings: large, noisy and out of equilibrium. *Nonlinearity*, 21:245–252, 2008.